Polymer Journal, Vol. 39, No. 7, pp. 712–721 (2007)

Preparations of Aromatic Diamine Monomers and Copolyamides Containing Phosphorylcholine Moiety and the Biocompatibility of Copolyamides

Yu NAGASE,[1,†] Masataka OKU,[1] Yasuhiko IWASAKI,[2] and Kazuhiko ISHIHARA[3]

[1]*Department of Applied Chemistry, Graduate School of Engineering, Tokai University, 1117 Kitakaname, Hiratsuka 259-1292, Japan*
[2]*Department of Chemistry and Materials Engineering, Faculty of Chemistry, Materials and Bioengineering, Kansai University, 3-3-35, Yamate-cho, Suita 564-8680, Japan*
[3]*Department of Material Engineering, School of Engineering, The University of Tokyo, 7-3-1 Hongo, Bunkyo-ku, Tokyo 113-8656, Japan*

(Received March 5, 2007; Accepted April 9, 2007; Published May 22, 2007)

ABSTRACT: The synthesis of a novel aromatic diamine compound containing phosphorylcholine (PC) group was carried out to prepare aromatic polyamides with PC moiety, in order to develop durable biocompatible polymer materials. The desired diamine compound, 2-(3,5-diaminophenylcarbonyloxy)ethyl phosphorylcholine (DAPC), was prepared from a reaction of 2-[2-(3,5-dinitrophenylcarbonyloxy)ethyl]-2-oxo-1,3,2-dioxaphospholane with trimethylamine, followed by the reduction of the dinitro group by H_2/Pd. The starting phospholane compound was synthesized by a condensation reaction of 2-hydroxyethyl 3,5-dinitrobenzoate with 2-chloro-2-oxo-1,3,2-dioxaphospholane. The polycondensation of DAPC with 4,4′-diamino-3,3′-dimethyldiphenylmethane and isophthaloyl chloride gave the copolyamides with different PC contents. From the results of contact angle of water and XPS analysis on the surface of the copolyamide coating films, it was found that PC units were concentrated on the surface after immersed in water. In addition, by using 2,2-bis[4-(aminophenyloxy)phenyl]propane or 2,2-bis[4-(aminophenyloxy)phenyl]hexafluoropropane as a diamine comonomer with DAPC, high molecular weight copolyamides containing PC moiety were obtained to prepare homogeneous coating films. The obtained copolyamides exhibited the high thermal stability, and also the excellent biocompatibility even though the content of PC monomer unit in the copolymer was around 20 mol %, which was confirmed by the platelet adhesion test. Therefore, the introduction of PC group in the side chain of aromatic polyamide was effective to develop the biocompatibility, which would be due to the surface property covered with polar PC units. [doi:10.1295/polymj.PJ2006253]

KEY WORDS Diamine Monomer / Aromatic Polyamide / Phosphorylcholine / Polycondensation / Copolymer / Surface Property / Biocompatibility /

The phosphorylcholine (PC) group is an important component of phospholipid molecules in cell membranes,[1] and it is well known that synthetic polymer materials containing PC group have been shown to exhibit excellent biocompatibility including blood compatibility.[2–8] It has been well known that the copolymers consisted of 2-methacryloyloxyethyl phosphorylcholine (MPC) unit, so-called MPC polymers, have been reported as ideal blood compatible and biocompatible materials.[5–11] The MPC was designed based on the inspiration from the outer surface of the cell membrane, *i.e.*, the biomembrane, which is mainly constructed of natural phospholipid molecules. The MPC polymers were synthesized by a conventional radical copolymerization of MPC with various other alkyl methacrylates such as butyl methacrylate.[8,9] Furthermore, the blood compatibility of MPC polymers was investigated in detail, and the applications to medical devices and other uses have been greatly advanced in these years.[12–19] For example, when the surface of MPC polymers was contacted with blood components, the number of platelets adhered on the polymer surface was effectively decreased with an increase of the MPC unit in the copolymers. In particular, the adhesion and the activation of platelets were completely suppressed on the surface of the MPC polymers when the composition of MPC unit was above 30 mol %, and the amount of plasma proteins adsorbed on the surface of MPC polymer film was clearly decreased.[8] Since PC group consists of a zwitterions, MPC polymers behave as an entire neutrality molecule and exhibited no interaction with specific ions in the living organism. Therefore, MPC polymers are very useful polymeric biomaterials not only in the biomedical field but also in the tissue engineering and bioengineering fields. Actually, MPC polymers are now widely applied for development of artificial organs[13–19] and drag delivery systems.[20–22]

†To whom correspondence should be addressed (Tel: +81-463-58-1211, Fax: +81-463-50-2012, E-mail: yunagase@keyaki.cc.u-tokai.ac.jp).

However, most of MPC polymers do not possess the enough durability to several solvents such as alcohols, the thermal stability and the mechanical strength, which were derived from the polymethacrylate type main chain structure. Then, if these physical properties of MPC polymers were improved satisfactorily while maintaining the excellent biocompatibility, novel biocompatible polymer materials could be developed. The purpose of this study is the syntheses of novel polymer compounds, which exhibit the excellent biocompatibility with the processability, the durability to solvents, the thermal stability and the mechanical strength, in order to create the practical biomaterials for several applications.

In the present study, the synthesis of a novel aromatic diamine monomer with PC group was carried out to prepare the aromatic polyamides containing PC group, the backbone component of which was durable as compared with that of MPC polymers. In general, the aromatic polyamides are insoluble in many solvents, thermally stable up to 300 °C and mechanically tough materials,[23,24] which are used in a lot of electric devices and motorcars. Therefore, as the second subject of this paper, we attempted to prepare aromatic polyamides containing PC group in the side chain by using a diamine monomer with PC unit, which would lead to new biocompatible polyamides derived from the characteristics of PC group. In addition, the physical properties such as solubility, thermal property, biological function as blood compatibility, and surface property of the obtained polyamides were investigated to reveal the possibility of a durable biocompatible polymer material.

EXPERIMENTAL

Materials

Tetrahydrofuran (THF) was refluxed with sodium and benzophenone until the color turned blue to remove moisture, and purified by distillation. Triethylamine and acetonitrile was freshly distilled over calcium hydride. Trimethylamine was purified by distillation from its aqueous solution. 2-Chloro-2-oxo-1,3,2-dioxaphospholane (COP) was purchased from Tokyo Kasei Chemical Co. and used as received. 4,4′-Diamino-3,3′-dimethyldiphenylmethane and isophthaloyl chloride was purchased from Tokyo Kasei Chemical Co. and purified by recrystallization from chloroform and hexane, respectively. Other chemicals were used without further purification.

Synthesis of 2-Hydroxyethyl 3,5-dinitrobenzoate (1)

Under an argon atmosphere, a solution of 10.0 g of 3,5-dinitrobenzoyl chloride (43.4 mmol) in 150 mL of THF was gradually added to a solution of 24.0 mL of ethylene glycol (430 mmol) and 60 mL of triethylamine dissolved in 340 mL of THF at 0 °C. The reaction mixture was stirred at room temperature for overnight, and then it was poured into an excess amount of distilled water. The mixture was extracted with chloroform, and the organic layer was dried over sodium sulfate. After the solvent was evaporated under reduced pressure, the product was purified by column chromatography on silica gel with hexane/ethyl acetate (1/2 by vol.) to give **1** as a yellow powder. Yield: 8.95 g (80.6%).

^{1}H NMR, δ (400 MHz, $CDCl_3$, ppm): 1.92 (1H, t, J = 5.61 Hz), 3.98 (2H, m), 4.54 (2H, m), 9.13 (2H, d, J = 2.20 Hz), 9.18 (1H, t, J = 2.20 Hz).

IR, ν (KBr, cm^{-1}): 3222 (–OH), 3045, 2879 (C–H), 1722 (C=O), 1627, 1595 ($-NO_2$), 1541 (C=C), 1334, 1078, 844, 723.

Synthesis of 2-[2-(3,5-Dinitrophenylcarbonyloxy)ethyl]-2-oxo-1,3,2-dioxaphospholane (2)

Under an argon atmosphere, 2.70 mL of 2-chloro-2-oxo-1,3,2-dioxaphospholane (29.3 mmol) was gradually added to a solution of 5.00 g of **1** (19.5 mmol) and 3 mL of triethylamine dissolved in 90 mL of THF at 0 °C. After stirring for 2 h at room temperature, the reaction mixture was poured into an excess amount of distilled water and then extracted with chloroform. The obtained organic layer was dried over sodium sulfate, and the solvent was evaporated under reduced pressure to obtain **2** as a pink powder. Yield: 6.01 g (85.0%).

^{1}H NMR, δ (400 MHz, $CDCl_3$, ppm): 4.34–4.50 (6H, m), 4.61 (2H, m), 9.17 (1H, t, J = 1.96 Hz), 9.20 (2H, d, J = 2.20 Hz).

IR, ν (KBr, cm^{-1}): 3107, 2974 (C–H), 1720 (C=O), 1587 ($-NO_2$), 1550 (C=C), 1360, 1290 (P=O), 1164, 1060, 931, 721.

Synthesis of 2-(3,5-Dinitrophenylcarbonyloxy)ethyl phosphorylcholine (3)

Under an argon atmosphere, 2.02 mL of trimethylamine (22.4 mmol) was added to a solution of 4.05 g of **2** (11.2 mmol) in 60 mL of acetonitrile at −30 °C, then the reaction vessel was sealed with a glass cap. After stirring at 60 °C for overnight, the reaction mixture was evaporated, and the obtained product was purified by recrystallization from acetonitrile to give **3** as a pink powder. Yield: 4.59 g (97.4%).

^{1}H NMR, δ (400 MHz, DMSO-d_6, ppm): 3.13 (9H, s), 3.51 (2H, d, J = 4.64 Hz), 4.02 (2H, m), 4.06 (2H, m), 4.51 (2H, t, J = 4.64 Hz), 8.96 (2H, d, J = 2.20 Hz), 9.06 (1H, t, J = 2.20 Hz).

IR, ν (KBr, cm^{-1}): 2893 (C–H), 1718 (C=O), 1602 ($-NO_2$), 1535 (C=C), 1353, 1230 (P=O), 1076 (N–CH_3), 856, 773, 731.

Synthesis of 2-(3,5-Diaminophenylcarbonyloxy)ethyl phosphorylcholine (DAPC)

5% Pd on charcoal powder (0.25 g, 0.10 mmol by Pd) was suspended in a solution of 2.50 g of **3** (5.95 mmol) dissolved in 60 mL of ethanol. The mixture was degassed under reduced pressure at −78 °C, and the vessel was filled with hydrogen gas. After stirring at room temperature for overnight, the Pd on charcoal was filtered off, and the solvent was distilled off under reduced pressure. Then, the product was purified by recrystallization from ethanol to give **DAPC** as a yellow powder. Yield: 2.15 g (92.1%).

^{1}H NMR, δ (400 MHz, DMSO-d_6, ppm): 3.15 (9H, s), 3.33 (4H, bs), 3.53 (2H, t, J = 4.64 Hz), 4.00 (2H, m), 4.10 (2H, m), 4.43 (2H, t, J = 4.64 Hz), 7.78 (1H, s), 7.82 (1H, s), 8.03 (1H, s).

IR, ν (KBr, cm^{-1}): 3199 (–NH_2), 2885 (C–H), 1718 (C=O), 1535 (C=C), 1477, 1228 (P=O), 1076, 966, 780, 733.

Preparations of CPAPC-1 Series

The preparation of **CPAPC-1a** listed in Table I is given as a representative example.

Under an argon atmosphere, 0.50 g of **DAPC** (1.38 mmol), 2.81 g of 4,4′-diamino-3,3′-dimethyldiphenylmethane (**DA-1**, 12.4 mmol) and 2.80 g of isophthaloyl chloride (13.8 mmol) were mixed in a flask, and the vessel was cooled to −78 °C. After 20 mL of *N*-methyl-2-pyrrolidinone (NMP) was added slowly, the mixture was stirred for 5 h with increasing temperature from −78 °C to room temperature. Then, pouring the reaction mixture into excess methanol provided the brown precipitate, which was collected by filtration and purified by reprecipitation from its NMP solution to excess methanol. Finally, the product was dried *in vacuo* to give **CPAPC-1a** as a brown powder. Yield: 4.72 g (93.5%).

^{1}H NMR, δ (400 MHz, DMSO-d_6, ppm): See Figure 1.

IR, ν (KBr, cm^{-1}): 3270 (N–H), 2860 (C–H), 1652 (C=O), 1508, 1436, 1301, 1228 (P=O), 1076 (N–CH_3), 1050, 813, 725, 696.

CPAPC-1b and **CPAPC-1c** were prepared by the similar procedures of the preparation of **CPAPC-1a** with changing the molar ratio of **DAPC** and **DA-1** as shown in Table I.

Preparation of PA-1

Under an argon atmosphere, 1.00 g of **DA-1** (4.42 mmol) and 0.90 g of isophthaloyl chloride (4.42 mmol) were mixed in a flask, and the vessel was cooled to −78 °C. After 9.0 mL of NMP was added slowly, the mixture was stirred for 4 h with increasing temperature from −78 °C to room temperature. Then, pouring the reaction mixture into excess methanol provided the brown precipitate, which was collected by filtration and purified by reprecipitation from its NMP solution to excess methanol. Finally, the product was dried *in vacuo* to give **PA-1** as a light brown powder. Yield: 1.54 g (97.7%).

^{1}H NMR, δ (400 MHz, DMSO-d_6, ppm): 2.21 (6H, s), 3.91 (2H, s), 7.08 (2H, d, J = 1.95 Hz), 7.13 (2H, s), 7.28 (2H, d, J = 1.95 Hz), 7.63 (1H, t, J = 7.08 Hz), 8.14 (2H, d, J = 7.08 Hz), 8.55 (1H, s), 9.96 (2H, s).

IR, ν (KBr, cm^{-1}): 3282 (N–H), 2860 (C–H), 1662 (C=O), 1506, 1303, 1234, 815, 696.

Synthesis of 2,2-Bis[4-(nitrophenyloxy)phenyl]propane (4a)

To a solution of 5.00 g of 2,2-bis(4-hydroxyphenyl)propane (21.9 mmol) in 65 mL of dimethylsulfoxide (DMSO), 6.18 g of 4-fluoronitrobenzene (43.8 mmol) and 6.05 g of potassium carbonate (43.8 mmol) and were added. After the mixture was stirred at r.t. for overnight, the reaction mixture was poured into excess water to precipitate the product. Then, the product was purified by recrystallization with chloroform/hexane to afford **4a** as a pale yellow powder. Yield: 9.64 g (87.7%).

^{1}H NMR, δ (400 MHz, DMSO-d_6, ppm): 1.70 (6H, s), 7.11 (8H, m), 7.36 (4H, m), 8.25 (4H, m).

Synthesis of 2,2-Bis[4-(aminophenyloxy)phenyl]propane (DA-2)

5% Pd on charcoal powder (0.50 g, 0.21 mmol by Pd) was suspended in a solution of 5.00 g of **4a** (10.6 mmol) dissolved in 50 mL of ethanol and 50 mL of THF. The mixture was degassed under reduced pressure at −78 °C, and the vessel was filled with hydrogen gas at over 760 mmHg. After stirring at room temperature for overnight, the Pd on charcoal was filtered off, and the solvents were distilled off under reduced pressure. Then, the product was purified by recrystallization from ethanol to give **DA-2** as a pale yellow powder. Yield: 3.80 g (86.8%).

^{1}H NMR, δ (400 MHz, DMSO-d_6, ppm): 1.52 (6H, s), 5.03 (4H, bs), 6.53 (4H, m), 6.67 (8H, m), 7.05 (4H, m).

Synthesis of 2,2-Bis[4-(nitrophenyloxy)phenyl]hexafluoropropane (4b)

4b was prepared by the similar procedure of the preparation of **4a** by using 2,2-bis(4-hydroxyphenyl)-hexafluoropropane instead of 2,2-bis(4-hydroxyphenyl)propane. Yield: 91.1%.

^{1}H NMR, δ (400 MHz, DMSO-d_6, ppm): 7.25 (8H, m), 7.47 (4H, m), 8.28 (4H, m).

Synthesis of 2,2-Bis[4-(aminophenyloxy)phenyl]hexafluoropropane (DA-3)

DA-3 was prepared by the similar procedure of the

preparation of **DA-2** by using **4b** instead of **4a**. Yield: 77.2%.
^{1}H NMR, δ (400 MHz, DMSO-d_6, ppm): 4.95 (4H, bs), 6.62 (4H, d, J = 7.81 Hz), 6.78 (4H, m), 6.88 (4H, m), 7.23 (4H, m).

Preparations of CPAPC-2 and CPAPC-3 Series

The preparations of **CPAPC-2a**, **CPAPC-2b**, **CPAPC-2c**, **CPAPC-3a**, **CPAPC-3b** and **CPAPC-3c** listed in Table II were carried out as the same procedure as the preparation of **CPAPC-1a** by using **DA-2** or **DA-3** instead of **DA-1** with changing the molar ratio of **DAPC** and **DA-2** or **DA-3**.
^{1}H NMR of **CPAPC-2a**, δ (400 MHz, DMSO-d_6, ppm): 1.65 (s, $-CH_3$), 3.11 (s, N$-CH_3$), 3.60 (m, $-CH_2-$), 4.24 (m, $-CH_2-$), 4.52 (m, $-CH_2-$), 6.89 (m, –Ph–), 6.99 (m, –Ph–), 7.21 (m, –Ph–), 7.64 (m, –Ph–), 7.81 (m, –Ph–), 7.95 (m, –Ph–), 8.13 (m, –Ph–), 8.39 (m, –Ph–), 8.49 (m, –Ph–), 8.56 (m, –Ph–), 8.74 (m, –Ph–), 8.87 (m, –Ph–), 10.4 (s, –NH–).
^{1}H NMR of **CPAPC-3a**, δ (400 MHz, DMSO-d_6, ppm): 3.12 (s, N$-CH_3$), 3.58 (m, $-CH_2-$), 4.20 (m, $-CH_2-$), 4.51 (m, $-CH_2-$), 7.05 (m, –Ph–), 7.34 (m, –Ph–), 7.67 (m, –Ph–), 7.88 (m, –Ph–), 7.96 (m, –Ph–), 8.15 (m, –Ph–), 8.39 (m, –Ph–), 8.48 (m, –Ph–), 8.57 (m, –Ph–), 8.73 (m, –Ph–), 8.87 (m, –Ph–), 10.51 (s, –NH–).

Preparation of PA-2 and PA-3

The preparations of **PA-2** and **PA-3** were carried out as the same procedure as the preparation of **PA-1** by using **DA-2** or **DA-3** instead of **DA-1**.
^{1}H NMR of **PA-2**, δ (400 MHz, DMSO-d_6, ppm): 1.62 (6H, s), 6.89 (4H, d, J = 8.54 Hz), 7.01 (4H, d, J = 8.79 Hz), 7.21 (4H, d, J = 8.55 Hz), 7.66 (1H, t, J = 7.82 Hz), 7.79 (4H, d, J = 9.03 Hz), 8.12 (2H, d, J = 7.32 Hz), 8.52 (1H, m), 10.4 (2H, s).
^{1}H NMR of **PA-3**, δ (400 MHz, DMSO-d_6, ppm): 7.05 (4H, d, J = 8.30 Hz), 7.13 (4H, d, J = 9.03 Hz), 7.33 (5H, m), 7.87 (4H, d, J = 8.30 Hz), 8.14 (2H, m), 8.55 (1H, m), 8.52 (1H, m), 10.4 (2H, s).

Characterizations

^{1}H NMR spectra were conducted with a JEOL NM-TH5SK 400 MHz FT-NMR spectrometer, and the chemical shifts were estimated in ppm units with tetramethylsilane (TMS) as an internal standard. Infrared (IR) spectra were recorded with a Shimadzu FT/IR-8400 spectrometer. The molecular weights of polymers were estimated by Tosoh gel permeation chromatography (GPC) system equipped with a pump of CCPD, three columns of TSK gels Multipore HXL-M, a column oven of CO-8010 and RI detector of RI-8010 in DMF eluent at 40 °C. Average molecular weights were evaluated by polystyrene standards. Differential scanning calorimetry (DSC) was carried out on a Seiko Instruments DSC-6200 under a nitrogen flow rate of 30 mL/min and a heating rate of 10 °C/min.

Surface Characterizations of Polymers

Circular pieces of poly(ethylene terephthalate) (PET) plates (diameter: 14 mm, thickness: 0.2 mm) were dipped in 0.5 wt % polymer solutions in NMP for 30 min, and the obtained polymer-coated PET plates were dried slowly at 60 °C for 2 h. This procedure was repeated three times, and then they were dried *in vacuo*. Contact angles of water on the surfaces of the polymer-coated PET plates were measured using an Erma contact-angle microscope at room temperature. On the other hand, X-ray photoelectron spectroscopy (XPS) was conducted on the surface of the polymer-coated PET plates by using ULVAC-PHI Quantum 2000 XPS apparatus. The take-off angle of the photoelectron was 45 degree.

Evaluation of Blood Compatibility

Whole blood was collected from healthy donors. In a polyethylene disposable syringe containing 3 mL of a 3.8 wt % aqueous sodium citrate solution, 30 mL of fresh blood was collected. The citrated whole blood was immediately centrifuged for 15 min at 1200 rpm to obtain citrated platelet-rich plasma (PRP).

The polymer-coated PET plates were contacted with phosphate-buffered solution (PBS, pH = 7.4) at r.t. for overnight to equilibrate the surface, then human whole blood or PRP was poured onto the plates and incubated for 60 min at 37 °C. After the incubation, whole blood and PRP were removed with an aspirator, and the plates were rinsed three times with PBS, and then 0.7 mL of 2.5 vol % glutaraldehyde in PBS was poured onto each plate, and the materials were maintained at room temperature for 2 h in order to fix the blood components on the plates. After the fixation, it had been rinsed five times with distilled water, and then the plate was freeze-dried. The surfaces of the polymer-coated plates were observed with a scanning electron microscope (SEM) by using JEOL JSM-5200 after a gold-sputtering treatment.

Measurement of the Amount of Platelets Adsorbed on the Polymer Surface

After incubating the polymer-coated plates in the above procedure, PRP was removed and the plates were washed 3 times with PBS and transferred into 0.5 wt % aqueous solution of polyethylene glycol mono-*p*-isooctylphenyl ether (Triton X100) to elute the adsorbed platelets. The concentration of platelets in the Triton X100 solution was counted by a lactate

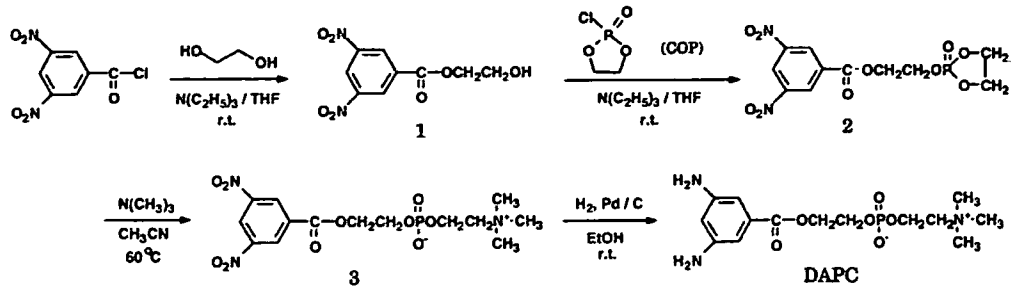

Scheme 1. Preparation of aromatic diamine monomer containing PC group (**DAPC**).

dehydrogenase (LHD) assay using an LDH-Cytotoxic Test Kit (Wako Chemicals, Osaka, Japan). The concentration of platelets in PRP was determined with a Coulter counter (MULTISIZER II, Beckman Coulter, CA) and the number of platelets that adhered on the polymer films was estimated based on the absorbance of the PRP-diluted system.

RESULTS AND DISCUSSION

Synthesis of a Diamine Monomer Containing PC Unit

The synthetic route of the novel aromatic diamine monomer containing PC group, 2-(3,5-diaminophenylcarbonyloxy)ethyl phosphorylcholine (**DAPC**), is outlined in Scheme 1. At first, the reaction of ethylene glycol with 3,5-dinitrobenzoyl chloride yielded a dinitro compound (**1**), which was obtained in good yield by using excess amount of ethylene glycol to 3,5-dinitrobenzoyl chloride. Next, the reaction of **1** with 2-chloro-2-oxo-1,3,2-dioxaphospholane (COP) yielded a dinitro-phospholane compound (**2**), which was an intermediate of phosphorylcholine compound. The purification of **2** by a silica-gel column chromatography was difficult because it was easily hydrolyzed. However, the extraction of the crude products with chloroform followed by washing with distilled water gave the pure product of **2**. Next, **DAPC** was obtained by opening the cyclic phosphoric ester moiety of **2** with trimethylamine, followed by the reduction of the nitro groups of **3** with H_2 catalyzed by Pd. The chemical structure of **DAPC** was confirmed by IR and ^{1}H NMR spectra. In the IR spectra of **DAPC**, a broad adsorption peak in the region of 3400–3150 cm^{-1} was observed as the amino groups, and the PC group was identified by the peak at 1228 and 1076 cm^{-1}. This novel aromatic diamine compound, **DAPC**, would be a useful monomer for the syntheses of various aromatic polymers, such as polyamides, polyimides, polyureas and poly(urethane-urea)s that have PC group in the side chain.

Preparation of Polyamides Containing PC Unit

In the case of MPC polymer, which was obtained by copolymerization of MPC monomer and butyl methacrylate, the adhesion and the activation of platelets were suppressed on the surface of the MPC polymer when the composition of MPC unit was above 30 mol %. Then, in this case, the synthesis of copolyamide was carried out, where the polycondensation of **DAPC** with acid chloride by coexisting another diamine comonomer. As the comonomer, 4,4′-diamino-3,3′-dimethyldiphenylmethane (**DA-1**) was used to make the polymer soluble in some solvents. Namely, the aromatic copolyamides containing PC group (**CPAPC-1**) were prepared by the low-temperature polycondensation of **DAPC** and **DA-1** with isophthaloyl chloride in NMP, as shown in Scheme 2. On the other hand, a homopolyamide (**PA-1**) without PC group was prepared from **DA-1** and isophthaloyl chloride to compare the physical properties with **CPAPC-1**.

Table I summarizes the results of polymerizations. Three copolyamides with different contents of PC unit were prepared by changing the amount of **DAPC** in the feed of copolymerization. The number-average molecular weights (M_n) of the obtained polyamides were in the ranges of 5×10^3–2×10^4. Figure 1 shows the ^{1}H NMR spectra of **CPAPC-1a**. The compositions of PC unit in **CPAPC-1** series were determined from the ratio of the peak intensities of the ammonium proton (3.08 ppm) of PC unit and methyl proton (3.89 ppm) of 3,3′-dimethyldiphenylmethane unit. In the IR spectra, the absorption peaks of the amide and ester groups were observed at 3270 cm^{-1} and 1652 cm^{-1}, respectively, and the PC group was identified from the peak at 1228 cm^{-1}.

On the other hand, to obtain the higher molecular weight polyamides with PC unit, different polyamides containing Bisphenol A components were prepared from other comonomers, 2,2-bis[4-(aminophenyloxy)-phenyl]propane (**DA-2**) and 2,2-bis[4-(aminophenyloxy)phenyl]hexafluoropropane (**DA-3**), which were expected to possess the higher reactivity than **DA-1**. These two comonomers, **DA-2** and **DA-3**, were synthesized in high yields by the procedure shown in Scheme 3 and the experimental section. Then, the

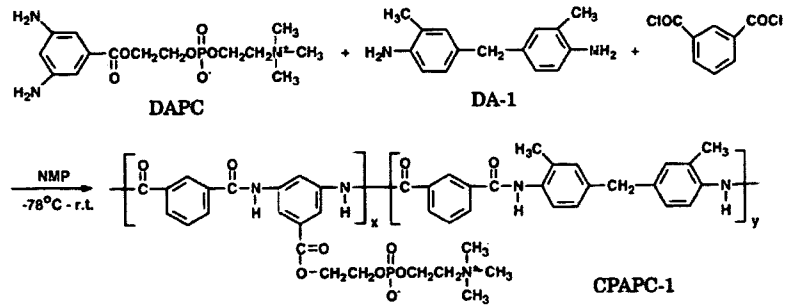

Scheme 2. Preparation of polyamide containing PC group (**CPAPC-1**).

Table I. Polymerization results of **CPAPC-1** series

Code	Composition (mol %)		Yield (%)	M_n[b] ($\times 10^4$)	M_w/M_n[b]	T_g[c] (°C)
	DAPC/DA-1	x/y in copolymer[a]				
CPAPC-1a	10/90	5/95	94	1.98	5.57	210
CPAPC-1b	20/80	12/88	73	1.00	5.24	186
CPAPC-1c	30/70	21/79	59	0.53	4.36	175
PA-1	0/100	0/100	98	2.02	3.06	187

a) Calculated from the ratio of peak intensities of ^{1}H NMR spectra. b) Number-average and weight-average molecular weight (M_n and M_w) were determined by GPC based on polystyrene standards. c) Determined by DSC measurement at a heating rate of 10 °C/min.

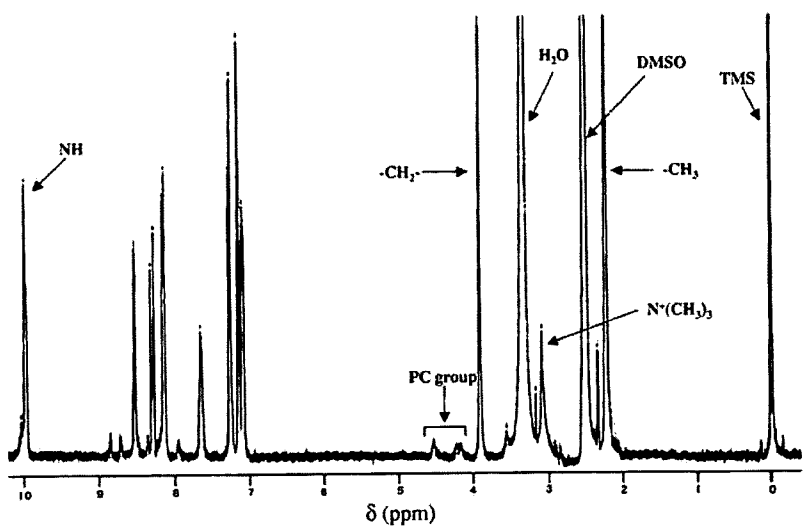

Figure 1. ^{1}H NMR spectrum of **CPAPC-1a**.

polycondensation of **DAPC** and **DA-2** or **DA-3** with isophthaloyl chloride yielded the desired copolyamides containing PC unit, **CPAPC-2** and **CPAPC-3**, as shown in Scheme 4. The results of polymerizations are summarized in Table II, where the homopolyamides, **PA-2** and **PA-3**, were polymerized of isophthaloyl chloride with **DA-2** and **DA-3**, respectively.

As seen in Tables I and II, the molecular weights of **CPAPC-2** and **CPAPC-3** series were higher than those of **CPAPC-1** series, which would be due to the higher reactivity of **DA-2** and **DA-3** than **DA-1**. However, in all the copolymers, the composition of PC component (x unit of the copolymers shown in Schemes 2 and 4) were lower than the molar composition of **DAPC** against **DA-1**, **DA-2** or **DA-3** in each polymerization, and the polymer yields decreased as the PC content increased. Therefore, the reactivity of **DAPC** in such a polycondensation would be relatively low, and the highly hygroscopic property of **DAPC** would disturb the polycondensation using a moisture-sensitive acid chloride. The molecular design of PC diamine monomer is now in progress to develop the higher reactivity.

The obtained **CPAPC** series exhibited a good solu-

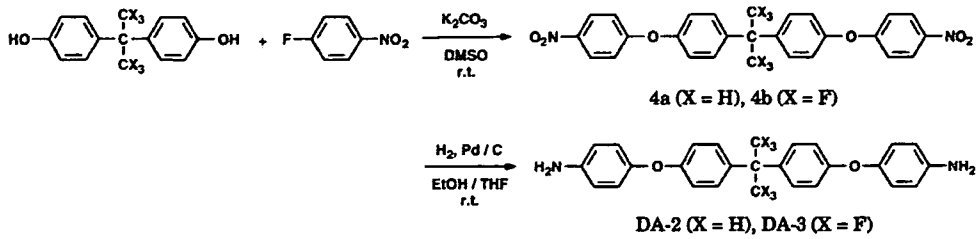

Scheme 3. Preparation of Bisphenol A type diamine monomers (**DA-2** and **DA-3**).

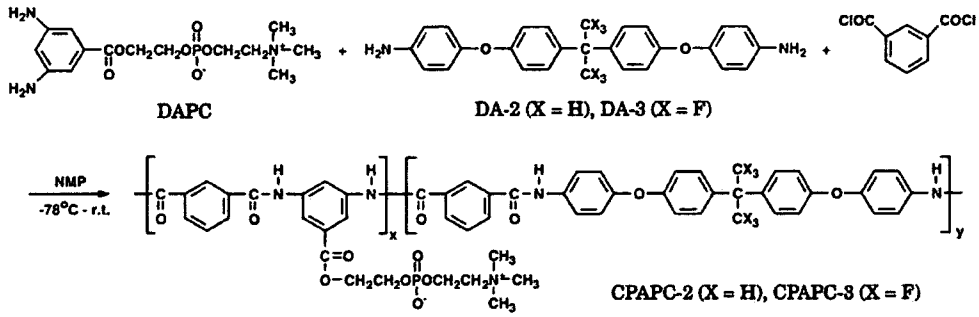

Scheme 4. Preparation of polyamides containing PC group (**CPAPC-2** and **CPAPC-3**).

Table II. Polymerization results of **CPAPC-2** and **CPAPC-3** series

Code	Composition (mol %)		Yield (%)	M_n[b] ($\times 10^4$)	M_w/M_n[b]	T_g[c] (°C)
	DAPC/DA-2 or DA-3	x/y in copolymer[a]				
CPAPC-2a	10/90	4/96	92	8.06	2.84	212
CPAPC-2b	20/80	7/93	82	3.71	4.46	210
CPAPC-2c	30/70	17/83	74	1.76	5.19	191
PA-2	0/100	0/100	99	10.8	2.86	215
CPAPC-3a	10/90	7/93	96	3.48	4.65	215
CPAPC-3b	20/80	10/90	80	2.68	5.98	210
CPAPC-3c	30/70	17/83	63	1.79	4.12	185
PA-3	0/100	0/100	97	19.3	1.92	212

[a]Calculated from the ratio of peak intensities of ^{1}H NMR spectra. [b]Number-average and weight-average molecular weight (M_n and M_w) were determined by GPC based on polystyrene standards. [c]Determined by DSC measurement at a heating rate of 10 °C/min.

bility in aprotic polar solvents such as NMP, DMF and DMSO at room temperature, whereas it was insoluble in several solvents such as methanol, ethanol, acetone, tetrahydrofuran and water. This solubility in the specific solvents is advantageous in the processing for medical devices, and the insolubility in other solvents enables the material durable to these solvents. The thermal property of **CPAPC** was evaluated by differential scanning calorimetry (DSC). As a result, **CPAPC** was a glassy polymer, the glass transition temperature (T_g) of which was in the range of 175–215 °C, as shown in Tables I and II. Such a thermal stability of **CPAPC** would be sufficient for the applications to biomaterials and medical devices, especially in the sterilization process.

Therefore, as compared with MPC polymer, it was found that the physical characteristics of **CPAPC** series were durable to common organic solvents such as alcohols and exhibited the higher softening temperature, whereas the MPC polymer were easily soluble in common organic solvents and softened at T_g of below 100 °C. In addition, the mechanical properties of **CPAPC** and MPC polymer films were quite different, where Young's moduli of **CPAPC-2a**, **PA-2** and MPC polymer were 248, 642 and 15.2 MPa, respectively. These physical properties of **CPAPC** series obviously depended on the aromatic polyamide backbone.

Surface Property of CPAPC

In order to clarify the effect of PC group on the surface of **CPAPC**, the surface analysis of the polymer

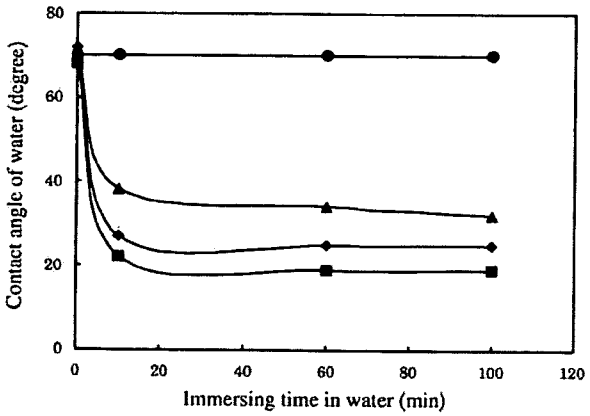

Figure 2. Effect of immersing the polymer coating films in water on the contact angle of water of the film surfaces. ●: **PA-1**, ▲: **CPAPC-1a**, ◆: **CPAPC-1b**, ■: **CPAPC-1c**

films was performed. Figure 2 shows the time-course of contact angle of water on the surface of polymer films after the films were immersed in water. In the case of **PA-1** without PC unit, the contact angle didn't change before and after immersed in water. On the contrary, the contact angles of the **CPAPC-1** films were significantly decreased after the films were immersed in water. Thus, the surface of the polymer membrane became hydrophilic by the introduction of PC unit and by contacting the surface with water. This result indicated that **CPAPC-1** membrane surfaces were largely swelled by water and the PC group of **CPAPC-1** was oriented to the water-side. The similar tendency was observed for **CPAPC-2** and **CPAPC-3** series.

Furthermore, the surface chemical structure of **CPAPC-1b** film before and after immersed in water for a day was analyzed by X-ray photoelectron spectroscopy (XPS), as shown in Figure 3. The XPS signals observed at 284, 288, 291, and 293 eV in C_{1s} region were attributed to carbon in hydrocarbons ($-CH_3$, $-CH_2-$), the ether bond (–C–O–C–), the carbonyl group [–C(=O)–], and aromatic carbon, respectively. The peaks which were observed at 531, 536, 399, 406, and 133 eV were attributed to the carbonyl group [–C(=O)–], oxygen of the ether bond (–O–), the nitrogen atoms in the amide bond (–NH–), the ammonium group ($-N^+(CH_3)_3-$), and phosphorus of the phosphate group, respectively. Therefore, the PC unit seems to be concentrated at the **CPAPC** film surface after immersed in water for a day, because the peaks derived from PC unit were obviously increased after contact with water. The chain rearrangement of the copolymer film surface would result in such a change of elemental distribution. In addition, it is expected that **CPAPC** series show the blood compatibility, because the film surface after immersed in water is very similar to a biomembrane surface which is covered with the polar group of phospholipid.

Biocompatibility of CPAPC

The thin films of **CPAPC-1a**, **CPAPC-1c** and **PA-1** were prepared by coating of the NMP solutions of the polymers on poly(ethylene terephthalate) (PET) plates, and the blood compatibility of the coating films was evaluated by contacting the plates with a human blood. Figure 4 shows SEM pictures of the **PA-1**, **CPAPC-1a** and **CPAPC-1c** film surfaces after contact with human whole blood and platelet-rich plasma (PRP) for 60 min. The numerous adherent blood cells and human platelets on the **PA-1** film surface were observed as large aggregates. In contrast, the blood cells and platelets were significantly suppressed on the **CPAPC-1a** and **CPAPC-1c** film surfaces as shown in Figure 4. These results clearly indicated that **CPAPC-1** series exhibited the excellent blood compatibility and PC unit in the copolyamide was an important element to develop the blood compatibility. Furthermore, the composition of the PC unit was a dominant factor in the reduction of the blood cell and platelet adhesion, which was revealed from the result that the number of adhered platelets was much decreased on **CPAPC-1c** film rather than **CPAPC-1a** film. These results would be due to the PC unit located at the surface of the polymer film, where the surface is covered with PC unit, and the interaction between the polymer surface and blood ingredients such as cells and platelets is very weak.

On the other hand, the homogeneous coating films without defects on PET plates were prepared from

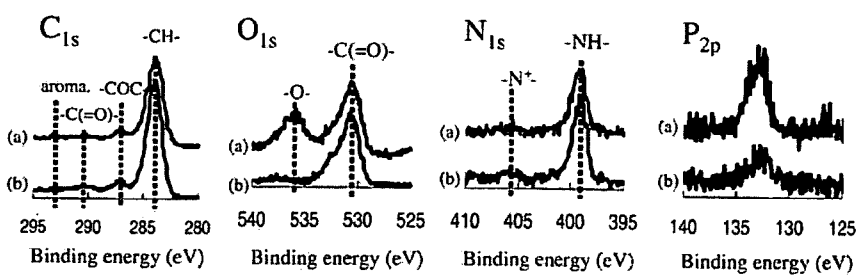

Figure 3. XPS spectra **CPAPC-1b** film surfaces before (b) and after (a) immersed in water for a day.

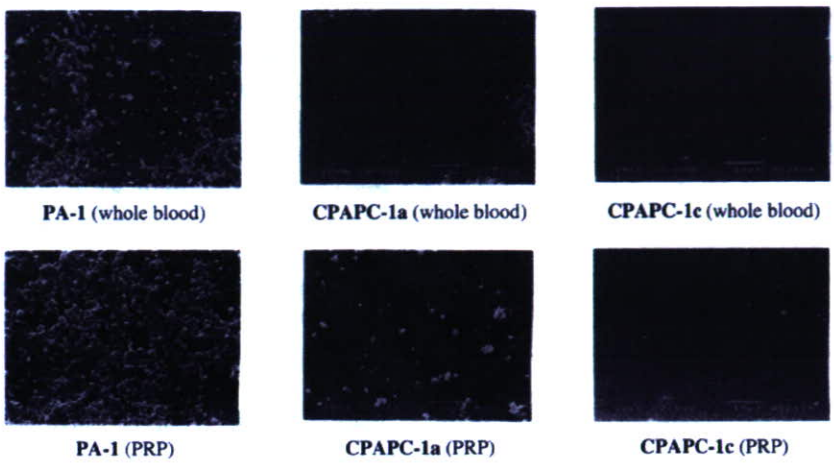

Figure 4. SEM pictures of polymer film surfaces after contact with human whole blood or PRP for 1 h (×1,000).

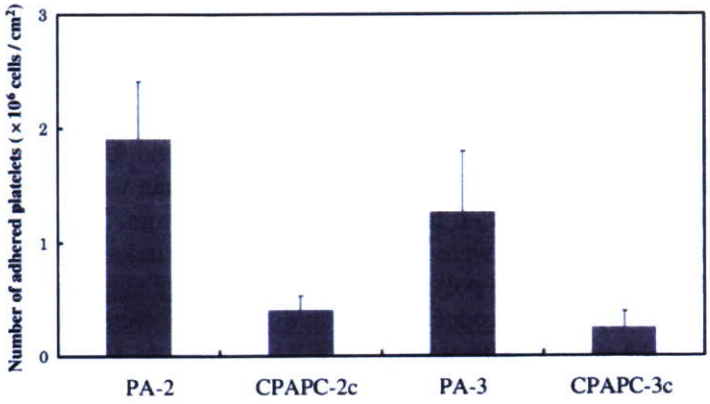

Figure 5. Number of adherent platelet on the polymer surfaces after contact with PRP for 1 h. Each bar represents mean ± S.E. for 4 experiments.

CPAPC-2 and **CPAPC-3** series, whereas the coating films from **CPAPC-1** series had some defects. Such a difference of the film forming ability of these PC copolyamides would be due to the difference of their molecular weights. Therefore, by using the coating films prepared from **CPAPC-2c** and **CPAPC-3c**, the platelets adhesion test was carried out as compared with **PA-2** and **PA-3** films. In the case of **CPAPC-1**, the platelets were remarkably adhered on the defects of coating film, thus, the quantitative results of the adhered platelets on **CPAPC-1** films were ambiguous. Figure 5 shows the number of platelets that adhered to polymer coating films after contact with PRP for 1 h. The number of adhered platelets on **CPAPC-2c**, **CPAPC-3c**, **PA-2** and **PA-3** films were 0.41, 0.25, 1.91 and 1.27 ($\times 10^6$ cells/cm^2), respectively. It was obvious that **CPAPC-2c** and **CPAPC-3c** films exhibited fewer adhered platelets than **PA-2** and **PA-3** films. These results indicated that the introduction of PC groups in these polyamides were very effective to enhance the biocompatibility, and the PC content of 17 mol % was enough to reduce the adhered platelets on the polymer surfaces. However, such a reduction of the adhered platelets on the MPC polymer film was more effective than the **CPAPC** series, where the number of adhered platelets on the MPC polymer surface was less than 10^5 cells/cm^2 in the same condition. Probably, the density of PC group on the surface of **CPAPC** series would be lower than that of MPC polymer, because of the rigidity of main chain structure of **CPAPC**.

CONCLUSION

Synthesis of a novel aromatic diamine compound containing PC group, **DAPC**, was carried out to prepare aromatic polyamides with PC moiety. The polycondensation of **DAPC** with other diamine compounds and isophthaloyl chloride gave the desired copolyamides with different PC contents. The obtained copolyamides were glassy polymers with high glass transition temperatures over 150 °C, and soluble in aprotic polar solvents but insoluble in many other solvents, the properties of which were derived from

the main chain rigid structure. Regarding the effects of PC group of these copolyamides on the blood compatibility, the introduction of such a polar group of phospholipid was effective to appear the blood compatibility even in the aromatic polyamide system. From the results of surface analyses of the copolyamide films, it was found that the PC group was easily rearranged by the immersion in water. Consequently, it is expected that the aromatic copolyamides containing PC group will be useful polymeric biomaterials to develop a new generation of biomedical devices, because of the different solubility, the higher thermal stability and the similar biocompatibility as compared to the MPC polymer.

However, the self-standing films were difficult to prepare from the copolyamides described in this paper except **CPAPC-2a**, thus, the mechanical property of the copolyamides could not be estimated in detail. To obtain the self-standing films, the main chain structure and the molecular weight of the copolyamides must be developed, which are now in progress.

Acknowledgment. This work was partially supported by a Grant-in-Aid for Scientific Research from the Ministry of Education, Culture, Sports, Science and Technology, Japan (No. 15550110).

REFERENCES

1. J. A. Hayward and D. Chapman, *Biomaterials*, **5**, 135 (1984).
2. K. Sugiyama, K. Ohga, H. Aoki, and N. Amaya, *Macromol. Chem. Phys.*, **196**, 1907 (1995).
3. T. Ohishi, T. Fukuda, H. Uchiyama, F. Kondou, H. Ohe, and H. Tsutsumi, *Polymer*, **38**, 3109 (1997).
4. Y. K. Gong, L. Luo, A. Petit, D. J. Zukor, O. L. Huk, J. Antoniou, F. M. Winnik, and F. Mwale, *J. Biomed. Mater. Res., Part A*, **72**, 1 (2005).
5. K. Ishihara, R. Aragaki, T. Ueda, A. Watanabe, and N. Nakabayashi, *J. Biomed. Mater. Res.*, **24**, 1069 (1990).
6. K. Ishihara, N. P. Ziats, B. P. Tierney, N. Nakabayashi, and J. M. Anderson, *J. Biomed. Mater. Res.*, **25**, 1397 (1991).
7. T. Ueda, H. Oshida, K. Kurita, K. Ishihara, and N. Nakabayashi, *Polym. J.*, **24**, 1259 (1992).
8. K. Ishihara, T. Ueda, and N. Nakabayashi, *Polym. J.*, **22**, 355 (1990).
9. K. Ishihara, H. Oshida, T. Ueda, Y. Endo, A. Watanabe, and N. Nakabayashi, *J. Biomed. Mater. Res.*, **26**, 1543 (1992).
10. S. Sawada, Y. Iwasaki, N. Nakabayashi, and K. Ishihara, *J. Biomed. Mater. Res., Part A*, **79**, 476 (2006).
11. J. Patel, Y. Iwasaki, K. Ishihara, and J. Anderson, *J. Biomed. Mater. Res., Part A*, **73**, 359 (2005).
12. Y. Iwasaki, A. Mikami, K. Kurita, N. Yui, K. Ishihara, and N. Nakabayashi, *J. Biomed. Mater. Res.*, **36**, 508 (1997).
13. T. Uchiyama, J. Watanabe, and K. Ishihara, *J. Membr. Sci.*, **210**, 423 (2002).
14. T. Moro, Y. Takatori, K. Ishihara, T. Konno, Y. Takigawa, T. Matsushita, U.-I. Chung, K. Nakamura, and H. Kawaguchi, *Nat. Mater.*, **3**, 829 (2004).
15. H. Ueda, J. Watanabe, T. Konno, M. Takai, A. Saito, and K. Ishihara, *J. Biomed. Mater. Res., Part A*, **77**, 19 (2006).
16. S.-H. Ye, J. Watanabe, M. Takai, Y. Iwasaki, and K. Ishihara, *Biomaterials*, **27**, 1955 (2006).
17. T. Goda and K. Ishihara, *Expert Rev. Med. Devices*, **3**, 167 (2006).
18. Y. Okajima, S. Saika, and M. Sawa, *J. Cataract. Refract. Surg.*, **32**, 666 (2006).
19. T. A. Snyder, H. Tsukui, S. Kihara, T. Akimoto, K. N. Litwak, M. V. Kameneva, K. Yamazaki, and W. R. Wagner, *J. Biomed. Mater. Res., Part A*, **81**, 85 (2007).
20. T. Konno, J. Watanabe, and K. Ishihara, *J. Biomed. Mater. Res., Part A*, **65**, 210 (2003).
21. K. W. Nam, J. Watanabe, and K. Ishihara, *Eur. J. Pharmacol.*, **23**, 261 (2004).
22. N. Chiba, M. Ueda, T. Shimada, H. Jinno, J. Watanabe, K. Ishihara, and M. Kitajima, *Eur. Sur. Res.*, **39**, 23 (2007).
23. P. E. Cassidy, "Thermal Stable Polymer," Dekker, New York, 1980, Chapter 4.
24. J. Preston, *Encycl. Polym. Sci. Eng.*, **11**, 381 (1988).

Available online at www.sciencedirect.com
ScienceDirect
Journal of Colloid and Interface Science 314 (2007) 446–459
JOURNAL OF Colloid and Interface Science
www.elsevier.com/locate/jcis

Polymer brushes in nanopores surrounded by silicon-supported tris(trimethylsiloxy)silyl monolayers

Voravee P. Hoven [a,*], Mayuree Srinanthakul [b], Yasuhiko Iwasaki [c], Ryoko Iwata [c], Suda Kiatkamjornwong [d]

[a] *Organic Synthesis Research Unit, Department of Chemistry, Faculty of Science, Chulalongkorn University, Phayathai Road, Pathumwan, Bangkok 10330, Thailand*
[b] *Program of Petrochemistry and Polymer Science, Faculty of Science, Chulalongkorn University, Phayathai Road, Pathumwan, Bangkok 10330, Thailand*
[c] *Institute of Biomaterials & Bioengineering, Tokyo Medical and Dental University, Tokyo 101-0062, Japan*
[d] *Department of Imaging and Printing Technology, Faculty of Science, Chulalongkorn University, Phayathai Road, Pathumwan, Bangkok 10330, Thailand*

Received 8 February 2007; accepted 29 May 2007
Available online 27 June 2007

Abstract

A chemically grafted tris(trimethylsiloxy)silyl (tris(TMS)) monolayer on a silicon oxide substrate was used as a template for creating nanoclusters of polymer brushes. Polymer brushes were synthesized by surface-initiated polymerization of 2-methacryloyloxyethyl phosphorylcholine (MPC) and *tert*-butyl methacrylate (*t*-BMA) via atom transfer radical polymerization (ATRP) from α-bromoester groups tethered to the residual silanol groups on the silicon surface after generating a range of tris(TMS) coverage. CuBr/bpy and CuBr/PMDETA were used as the catalytic system for PMPC and P*t*-BMA synthesis, respectively. The percentage of tris(TMS) coverage significantly influenced the thickness and morphology of the polymer brushes. Protrusions representing self-aggregation of PMPC brushes in nanopores as visualized by AFM analysis evidently suggested that PMPC brushes were distributed nanoscopically on the surface. The protrusion size and surface roughness corresponded quite well with the graft density of PMPC brushes. The fact that P*t*-BMA brushes grown from nanopores were almost featureless implies that self-aggregation of PMPC brushes is truly a consequence of phase incompatibility between hydrophilic PMPC brushes and hydrophobic tris(TMS). The antifouling characteristic of PMPC brushes, inferred from plasma protein adsorption, was subsequently varied by controlling the surface coverage ratio between PMPC brushes and tris(TMS).

Keywords: Polymer brush; Phospholipid polymer; Surface-initiated polymerization; Atom transfer radical polymerization; Nanoscale template

1. Introduction

Surface-tethered polymer brushes are well recognized as a novel route for producing polymeric thin films that are useful for several commercially important technologies, ranging from biotechnology to advanced microelectronics. They are defined as an assembly of polymer chains having one end attached to a surface or interface [1,2]. Tethering is sufficiently dense that the polymer chains are crowded and forced to stretch away from the surface or interface to avoid overlapping, sometimes much further than the typical unstretched size of a chain [3]. Surface-initiated polymerization (SIP) has been introduced as a potential tool to generate surface-tethered polymer brushes [4–6]. SIP, also called the "grafting from" method, holds advantages over the "grafting to" method where the process suffers an entropic barrier due to crowding of initial grafting polymer chains that prevent further insertion of polymer onto the surface, leading to relatively low graft density. The "grafting from" method, on the other hand, involves a stepwise growth of polymer chains from the surface by insertion of monomers. This allows better control over the polymer chain length and graft density. SIP coupled with "living radical polymerization" has proven to be the most popular method for creating surface-tethered polymer brushes [7–15]. By using these techniques, the molecular weight, molecular weight distribution as well as

* Corresponding author. Fax: +66 2218 7598.
E-mail address: vipavee.p@chula.ac.th (V.P. Hoven).

0021-9797/$ – see front matter
doi:10.1016/j.jcis.2007.05.088

architecture of the target polymer can be well controlled. Due to the versatility of the process for a wide range of readily available monomers, both chemical and physical properties of surface-tethered polymer brushes can be broadly tailored.

Artificially designed fine patterning of polymer thin films has received a great deal of attention in various fields of science and technology such as microelectronics, anti-etching optical devices, biological and chemical sensors, and tissue engineering. Moreover, their relevance as model heterogeneous systems has led to fundamental understanding of interface phenomena. This growing field has produced a variety of surface patterns at both nanometer and micrometer scales. At present, there are a few methods available for patterning thin films of surface-tethered polymer brushes. These include procedures based on photolithography [16–18], templating the deposition of polymers using patterned self-assembly monolayers (SAMs) [19,20], microcontact printing [21–23], and nanophase separation of block copolymers [24,25].

Recently, Fadeev and McCarthy [26] have introduced silicon-supported tris(trimethylsiloxy)silyl (tris(TMS)) monolayers as templates for the synthesis of binary monolayers of organosilanes on oxidized silicon wafers. By controlling the kinetics of the reaction between silanol groups on the silicon oxide surface with tris(trimethylsiloxy) chlorosilane (tris(TMSCl)), surfaces having a range of tris(TMS) coverage can be prepared. The incomplete reaction between the sluggish tris(TMSCl) and the silicon oxide surface allows a mixed tris(TMS)/silanol surface to be formed. Contact angle studies using probe fluids of different sizes showed that even closely packed monolayers of bulky tris(TMS) have interstitial holes, called "nanopores," that can be filled with organosilanes that are smaller than the cross-sectional area of the pores ($\sim$0.5 nm^2). Stafford and co-workers [27] have demonstrated that the unreacted silanol groups in the nanopores were capable of adsorbing carboxyl-terminated polystyrene (PS–COOH). The thickness of the adsorbed layer could be controlled by the tris(TMS) surface coverage, adsorbing solvent, and polymer molecular weight. Later, Jia and McCarthy [28] fabricated nanosized silicon oxide using the silicon-supported tris(TMS) monolayers as a template and tetrachlorosilane and water as precursors. After the removal of the organic tris(TMS) template by chemical etching, then hydrophilic silica surfaces with controlled nanoscale roughness can be generated. The subsequent chemisorption of tridecafluoro-1,1,2,2-tetrahydrooctyldimethylchlorosilane gave rise to hydrophobic surfaces.

This research aims to use the silicon-supported tris(TMS) monolayers as a template for creating polymer brushes having a nanoscale distribution. An organosilane carrying initiating site for SIP is chemically bound to the residual silanol groups in the nanopores of the substrate. The mixed tris(TMS)/initiating site monolayers are then subjected to SIP of the selected monomers, 2-methacryloyloxyethyl phosphorylcholine (MPC) and *tert*-butyl methacrylate (*t*-BMA), which are chosen as representatives of hydrophilic and hydrophobic monomers, respectively. In light of its compatibility with a variety of functional monomers, atom transfer radical polymerization (ATRP) is adopted as a living synthetic route for SIP of both monomers. The correlation between the graft density of polymer brushes, which is inversely proportional to tris(TMS) coverage, and surface topography is explored. We anticipate that a chemically grafted mixed monolayer of tris(TMS)/silanol groups can be used as nanometer-scale template for controlling the graft density of both hydrophobic and hydrophilic polymer brushes, as well as tuning surface topography and properties of the material's surface at the nanoscopic level.

2. Materials and methods

2.1. Materials

Silicon wafer (100 orientation, P/B doped, both single-side and double-side polished) were purchased from Siltron Inc., Korea. Tris(trimethylsiloxy) chlorosilane (tris(TMSCl)) was obtained from Gelest, USA. Anhydrous toluene (99.8%) and N,N,N',N',N''-pentamethyldiethylenetriamine (PMDETA, 99%) were purchased from Aldrich, USA and used as received. *tert*-Butyl methacrylate (*t*-BMA, 99%) obtained from Aldrich was distilled under reduced pressure prior to use. Copper(I) bromide (CuBr, 98%) 2,2′-bipyridyl, and ethyldiisopropylamine were supplied from Fluka, Switzerland. 2-Methacryloyloxyethyl phosphorylcholine (MPC) was purchased from NOF Corporation, Japan. Synthesis of 3-(2-bromoisobutyryl)alkyl dimethylethoxysilane and propyl-2-bromoisobutyrate were performed according to the modified method described in the literature [8] using dimethylethoxysilane and 1-propanol as substrates, respectively. Ultrapure distilled water was obtained after purification using a Millipore Milli-Q system (USA) that involves reverse osmosis, ion exchange and a filtration step. Other chemicals were of analytical grade, purchased from Merck, Germany, and used without further purification.

2.2. Characterization

The molecular weight and molecular weight distribution of the PMPC homopolymer were determined by a Tosoh gel permeation chromatography (GPC) system (Japan) with a refractive index detector and size exclusion columns, Shodex SB-804 HQ and SB-806 HQ; with poly(ethylene glycol) standards in distilled water containing 10 mM LiBr. The molecular weight and molecular weight distribution of the P*t*-BMA homopolymer were determined by a Waters gel permeation chromatography (GPC) system (USA) equipped with HR4, HR3, and HR1 THF columns connected to the refractive index detector, using THF as the eluent and polystyrene standards. ^{1}H NMR spectra were recorded in $CDCl_3$ using a Varian, model Mercury-400 nuclear magnetic resonance spectrometer (USA) operating at 400 MHz. AFM images were recorded with an atomic force microscope model SPI-3800, Seiko I (Japan). Measurements were performed in air using the tapping mode. Silicon nitride tips with a resonance frequency of 13 kHz and spring constants of 0.02–0.1 N/m were used. X-ray photoelectron spectra were collected at 15° take-off angle (between the plane of the surface and the entrance lens of the detector optics) using

a Scienta ESCA 200 spectrometer (Sweden) with Al$K\alpha$ X-rays. The thickness of polymer brushes was measured by an L115C Wafer™ Ellipsometer operating with a 70° incidence angle at 632.8 nm. The calculation was based on the refractive indices: $N_{\text{initiator}} = 1.443$, $N_{\text{MPC}} = 1.488$, $N_{t\text{-BMA}} = 1.460$, $N_{\text{hydroxyl}} = 1.462$, $N_{\text{tris(TMS)}} = 1.386$, and $N_{\text{substrate}} = 3.858$. A contact angle goniometer model 100-00 equipped with a Gilmont syringe and a 24-gauge flat-tipped needle (Ramé-Hart, Inc., USA) was used for the determination of contact angles. Dynamic advancing and receding angles were recorded while water was added to and withdrawn from the drop, respectively. The reported angle is an average of five measurements taken at different locations on each sample.

2.3. Pretreatment of silicon substrates

Silicon wafers were cut into 1.5 × 1.5 cm^2 substrates. The substrates, held in a slotted hollow glass cylinder (custom designed holder), were put in a freshly prepared mixture of 7 parts of concentrated H_2SO_4 and 3 parts of 30% H_2O_2. Substrates were submerged in the solution at room temperature for 2 h, rinsed with five to seven aliquots of deionized water and placed in a clean oven at 120 °C for 2 h. The silanization reaction was carried out immediately after treating the substrates in this fashion.

2.4. Preparation of silicon-supported mixed tris(TMS)/silanol monolayers

Cleaned and dried silicon substrates held in a slotted hollow glass cylinder were covered with 10 ml of anhydrous toluene containing ethyldiisopropylamine (0.17 ml, 1.0 mmol) in a Schlenk flask. Tris(trimethylsiloxy)chlorosilane (tris(TMSCl)) (0.35 ml, 1.0 mmol) was added by a syringe. Reactions were carried out at 60–70 °C for a predetermined period of time (24–96 h) under a nitrogen atmosphere. The substrates were rinsed with 1 × 10 ml of toluene, 2 × 10 ml of 2-propanol, 2 × 10 ml of ethanol, 1 × 10 ml of ethanol–water (1:1), 1 × 10 ml of water, and 1 × 10 ml of ethanol and were then dried in an oven at 120 °C for 10 min.

2.5. Preparation of silicon-supported α-bromoisobutyrate monolayers and silicon-supported mixed tris(TMS)/α-bromoisobutyrate monolayers

Cleaned and dried silicon substrates or silicon-supported mixed tris(TMS)/silanol monolayers held in a slotted hollow glass cylinder were covered with 10 ml of anhydrous toluene containing ethyldiisopropylamine (0.17 ml, 1.0 mmol) in a Schlenk flask. 3-(2-Bromoisobutyryl)alkyl dimethylethoxysilane (0.15 mmol) was added by a syringe. Reactions were carried out under a nitrogen atmosphere at ambient temperature for a varied reaction time. The substrates were rinsed with 1 × 10 ml of toluene, 2 × 10 ml of 2-propanol, 2 × 10 ml of ethanol, 1 × 10 ml of ethanol–water (1:1), 1 × 10 ml of water and 1 × 10 ml of ethanol and dried under vacuum.

2.6. Surface-initiated polymerization of 2-(methacryloyloxyethyl phosphorylcholine) (MPC)

A mixed solvent of 4:1 methanol:water (v/v) was used as a solvent for polymerization. The solvent was distilled and degassed by two freeze-pump-thaw cycles and purged with nitrogen gas to eliminate oxygen before use. CuBr (29 mg, 0.20 mmol) and 2,2′-bipyridyl (63 mg, 0.40 mmol) were dissolved in a Schlenk flask containing 12 ml of methanol. The solution was stirred under nitrogen at 0 °C before 6 ml of ultrapure distilled water was added. Then, propyl-2-bromoisobutyrate (12.6 mg, 0.06 mmol) was added as "sacrificial" initiator. After stirring for 30 min under a nitrogen atmosphere, the silicon-supported α-bromoisobutyrate monolayers or silicon-supported mixed tris(TMS)/α-bromoisobutyrate monolayers held in a slotted hollow glass cylinder were then submerged into the flask. MPC (3.6 g, 12 mmol) was dissolved separately in 12 ml of methanol and purged with nitrogen for 1 h. The MPC solution was added into the flask and polymerization was carried out at ambient temperature while stirring under a nitrogen atmosphere. The silicon substrates were then removed from the polymerization mixture after the desired reaction time and rinsed with copious amounts of methanol and water, respectively, before being Soxhlet-extracted by methanol for 48 h and dried under vacuum. PMPC formed in the solution from the "added" initiator was precipitated in cold THF. The viscous PMPC was re-dissolved in deionized water. The PMPC solution was passed through a silica column to remove the copper catalyst before it was subjected to dialysis and freeze-dried.

2.7. Surface-initiated polymerization of tert-butyl methacrylate (t-BMA)

Anhydrous toluene used as a solvent for polymerization was degassed by two freeze-pump-thaw cycles and purged with nitrogen gas to eliminate oxygen before use. CuBr (29 mg, 0.20 mmol) and PMEDTA (41.8 μl, 0.20 mmol) were dissolved in a Schlenk flask containing 15 ml anhydrous toluene. The solution was stirred under a nitrogen atmosphere at 0 °C. Then, propyl-2-bromoisobutyrate (12.6 mg, 0.060 mmol) was added as a "sacrificial" initiator. After stirring for 30 min under a nitrogen atmosphere, the silicon-supported α-bromoisobutyrate monolayers or silicon-supported mixed tris(TMS)/α-bromoisobutyrate monolayers held in a slotted hollow glass cylinder were then submerged into the flask. *t*-BMA (1.95 ml, 12 mmol) was dissolved separately in 15 ml anhydrous toluene and purged with nitrogen for 1 h. The *t*-BMA solution was transferred to the flask and polymerization was carried out at 90–100 °C while stirring under a nitrogen atmosphere. The silicon substrates were then removed from the polymerization mixture after the desired reaction time and rinsed with copious amounts of toluene, before being Soxhlet-extracted by toluene for 48 h and dried under vacuum. The solution containing P*t*-BMA formed from the "added" initiator was passed through a silica column to remove the copper catalyst. Solid P*t*-BMA was obtained after toluene was removed under reduced pressure.

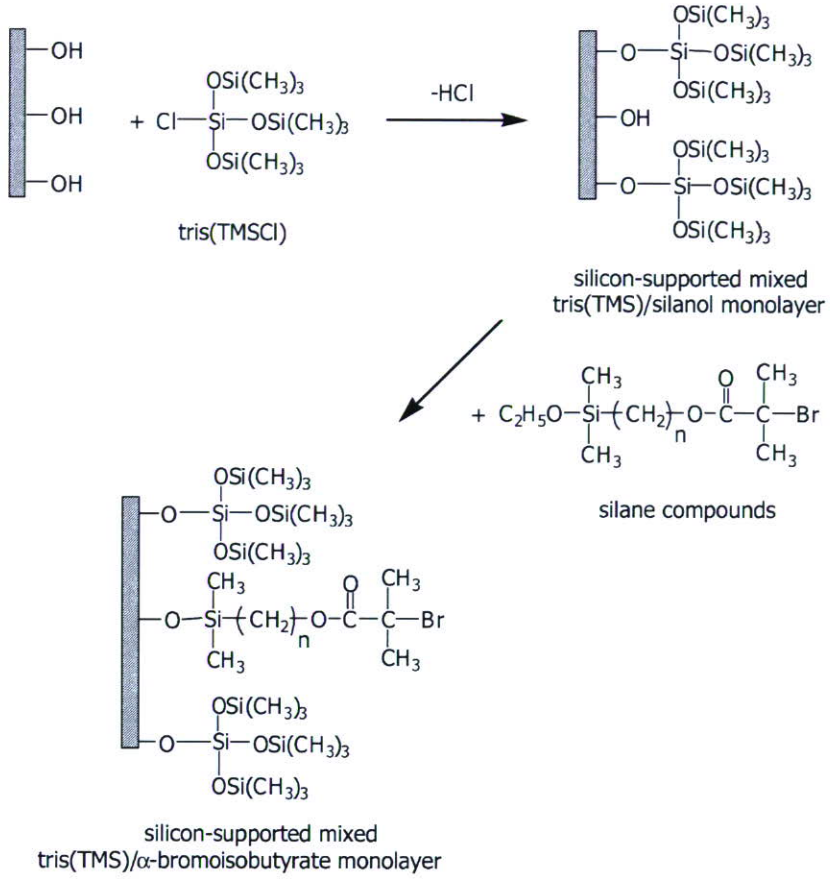

Scheme 1. Preparation of silicon-supported mixed tris(TMS)/α-bromoisobutyrate monolayer.

2.8. Determination of total amount of adsorbed human plasma protein

The silicon substrates having dimensions of 1.5 × 1.5 cm^2 were placed into a 24-well tissue culture plate containing ultrapure distilled water in each well. The samples were allowed to stand in the wells overnight to reach an equilibrium hydration. Each sample was removed from ultrapure distilled water and suspended in a well containing 3.0 ml platelet-poor plasma (PPP, Thai Red Cross Society, Thailand) before being incubated at 37 °C for 3 h. Three samples were analyzed for each condition. The samples were removed from PPP and rinsed thoroughly with phosphate buffer saline solution (PBS, Aldrich, USA) (2×) to remove any loosely attached protein. The adsorbed protein on the sample surface was detached by soaking each sample in 3.0 ml of 1% aqueous solution of sodium dodecyl sulfate (SDS, Fluka, Switzerland) for 30 min. A protein analysis kit based on the bicinchoninic acid method (Quanti-Pro™ BCA assay, Sigma, USA) was used to determine the concentration of the protein dissolved in the SDS solution. 100 μl (0.1 ml) of SDS solution that soaked each sample was added into a well of 96-well tissue culture plate. 100 μl of BCA working solution was then added in each well, before the well-plate was incubated at 37 °C for 2 h. The absorbance of the solution was measured at 562 nm by UV–Vis spectroscopy (Microtiter plate reader; model Sunrise, Tecan Austria GmbH). The amount of protein adsorbed on the samples was calculated from the protein concentration in the SDS solution by comparison of the absorbance of the samples with a calibration curve. Three repetitions were performed for all samples. The data are expressed as mean ± standard deviation (SD).

3. Results and discussion

3.1. Preparation of silicon-supported mixed tris(TMS)/α-bromoisobutyrate monolayers

Monolayers of tris(trimethylsiloxy)silyl (tris(TMS)) were prepared by the reaction between tris(trimethylsiloxy)chlorosilane (tris(TMSCl)) and silanol groups on a silicon substrate (Scheme 1, step 1). By controlling the kinetics of this reaction, a series of mixed monolayers of tris(TMS)/silanol having different surface coverages of tris(TMS) was prepared. The reaction kinetics can be monitored by contact angle analysis (Table 1). Initially there was a rapid rise in the contact angle of the cleaned silicon surface from ~0° to 62°/43° within 12 h, followed by a gradual increase over a period of 12–96 h, indicating that the surface became more hydrophobic as the tris-TMS coverage was increased. The contact angle of 92°/82° and the ellipsometric thickness of ~20 Å of the tris(TMS) layer were reached at 96 h.

Table 1
Water contact angle and calculated % coverage of the tris(TMS) monolayer as a function of reaction time

Reaction time (h)	Water contact angle (θ_A/θ_R)	%tris(TMS) coverage
12	62°/43°	51
24	73°/65°	66
48	81°/71°	75
72	86°/78°	82
96	92°/82°	87

Table 2
XPS atomic composition and contact angle data for the silicon-supported mixed tris(TMS)/α-bromoisobutyrate monolayers using a 96 h reaction time

%tris(TMS) coverage	XPS atomic concentration (%)				Br/C (%)	Water contact angle (θ_A/θ_R)
	Si	O	C	Br		
0	19.37	31.24	48.52	0.87	1.79	72°/68°
66	39.49	34.25	25.87	0.39	1.51	73°/52°
75	39.97	32.84	26.82	0.37	1.38	75°/55°
82	37.66	27.31	34.57	0.46	1.33	80°/63°

The degree of tris(TMS) coverage was determined from contact angle data according to the method proposed by Israelachvili and Gee for molecularly mixed heterogeneous surfaces [29]. The observed contact angle, θ_{obs}, can be described in terms of the mole fractions of each component, f_1 and f_2, as well as the contact angles for the pure surface of each component, θ_1 and θ_2, by

$$[1+\cos\theta_{obs}]^2 = f_1[1+\cos\theta_1]^2 + f_2[1+\cos\theta_2]^2, \quad (1)$$

$$f_1 + f_2 = 1. \quad (2)$$

In this study, the surface was treated as a mixture of tris(TMS) groups ($\theta_1 = 108°$) and silanol groups ($\theta_2 = 0°$) [26]. It should be noted that the advancing contact angle was used for θ_{obs} in all cases while f_1 and f_2 are defined as the mole fractions of tris(TMS) and silanol groups on the surface, respectively. The tris(TMS) coverage calculated using (1) and (2) is shown in Table 1.

Our results are in good agreement with those formerly reported [26]. However, it should be noted that the silanization in this study was carried out in the solution phase. As a result, our tris(TMS) monolayer is not as dense as those obtained using the vapor phase reaction. According to Fadeev and McCarthy, the vapor phase reaction after 72 h yielded tris(TMS) coverage of 91%, whereas 72% coverage was obtained in the solution phase reaction for the same duration. As a result of the bulky tris(TMS) groups, the reaction reaches its maximum extent as soon as the area occupied by unreacted silanol groups is too small for tris(TMSCl) to access. This assumption is supported by the fact that the contact angle tends to level off after 96 h, at which the maximum 87% tris(TMS) coverage has been reached (data not shown). These residual silanol groups, not blocked by tris(TMS), should be reactive sites available for further chemisorption. In our case, the unreacted silanol groups in the binary monolayer mixture of tris(TMS)/silanol were allowed to react with silane compounds having α-bromoester groups. The resulting binary monolayer mixture of tris(TMS)/α-bromoester was then used as a template for surface-initiated polymerization of vinyl monomers. Although Fadeev and McCarthy have mentioned that no size-exclusion contact angle hysteresis was found for the tris-TMS monolayer (of lower degree of surface coverage) prepared by liquid-phase silanization implying the absence of nanopores (as small as ~0.5 nm^2), our subsequent topographical investigation using AFM analysis suggests that the pores generated by liquid-phase silanization in this particular case are still in the nanometer range.

The silicon-supported mixed tris(TMS)/α-bromoisobutyrate monolayers were prepared by subsequent silanization of the silicon-supported mixed tris(TMS)/silanol monolayers having varied %tris(TMS) coverage with a silane compound having end-functionalized α-bromoisobutyrate (Scheme 1, step 2). The silane used for the investigation was 3-(2-bromoisobutyryl)propyl dimethylethoxysilane ($n = 3$), unless otherwise specified. It contains a bromine atom, which is not present in the tris(TMS) monolayers, so the formation of silicon-supported mixed tris(TMS)/α-bromoisobutyrate monolayers can easily be monitored by XPS analysis. These data can also be used to estimate the chemical composition of binary monolayer mixtures. XPS and contact angle data for the binary monolayer mixtures of tris(TMS)/α-bromoisobutyrate are summarized in Table 2. As determined from contact angle analysis (data are not shown), a period of 96 h was sufficient for the graft density of α-bromoisobutyrate groups to attain its maximum value regardless of %tris(TMS) coverage.

As expected, the data indicated that the percentage of Br/C decreased as the amount of tris(TMS) coverage increased. In other words, there are fewer α-bromoisobutyrate groups available for initiating ATRP of monomers when the content of tris(TMS) on the surface is elevated. Therefore, one can use these binary monolayer mixtures of tris(TMS)/α-bromoisobutyrate as templates for controlling the graft density of polymer brushes. Evidently, the advancing water contact angle of the silicon-supported mixed tris(TMS)/α-bromoisobutyrate monolayer increased as a function of %tris(TMS) coverage, similar to what was previously observed in the case of the silicon-supported mixed tris(TMS)/silanol monolayer.

3.2. *Surface-initiated polymerization on silicon-supported α-bromoisobutyrate monolayer*

Poly(2-methacryloyloxyethyl phosphorylcholine) (PMPC) is of particular interest, mainly due to its favorable non-fouling characteristic, meaning that it resists non-specific interactions with proteins and cells [30,31] and the activation and inflammatory responses of cells are not induced in contact with MPC polymers [32,33]. Formation of PMPC brushes by surface-initiated ATRP was first reported on anionic silicon sol surfaces by Chen and Armes [34] and later by Feng and co-workers [35]. They have indicated that the growth of PMPC brushes can be controlled by addition of a free initiator as well as a deactivator. The living characteristic of the PMPC brushes was verified by the success in extending the second block of the same monomer or 2-(dimethylamino)ethyl methacrylate. Iwata and co-workers [36] independently reported the synthesis of the same polymer brush system. They have succeeded in using the

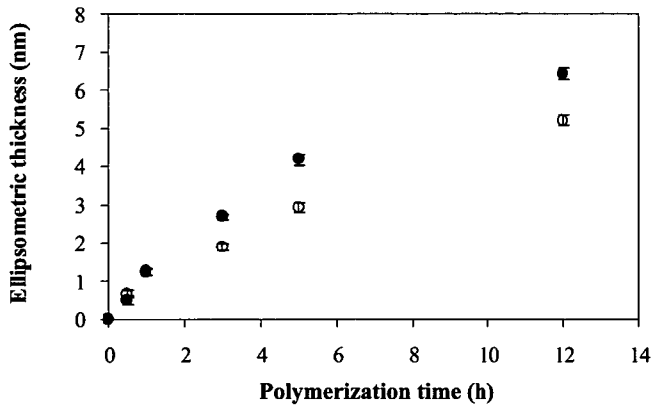

Fig. 1. Ellipsometric thickness of polymer brushes versus polymerization time for targeted DP = 200: (●) PMPC and (○) P*t*-BMA.

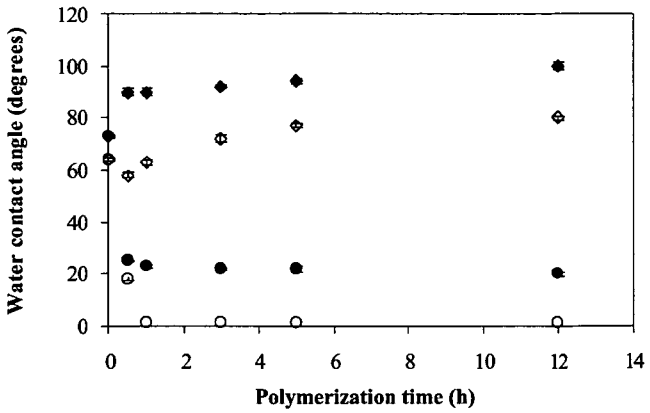

Fig. 2. Water contact angle data of polymer brushes versus polymerization time for PMPC: (●) θ_A, (○) θ_R and P*t*-BMA: (◆) θ_A, (◇) θ_R.

micropatterned surface-tethered PMPC brushes to manipulate proteins and cells. Evidently, the bovine serum albumin and fibroblast cells selectively adhered on the areas where there was an absence of PMPC brushes having a thickness greater than 5.5 ± 1.0 nm.

Later, Feng and co-workers have investigated the adsorption of proteins on the PMPC brushes. They have found that the suppression of protein adsorption from protein mixtures (fibrinogen and lysozyme) was not strongly dependent on protein size and charge [37]. Also, the effect of the graft density of the PMPC brushes on the adsorption of fibrinogen was more profound than that of the chain length [38]. To control the graft density of PMPC brushes, they have used silicon substrates having a mixed composition of α-bromoester groups (initiating sites) and alkyl groups (diluting groups) through a competitive chemisorption of 10-(2-bromo-2-methyl)propionyloxydecyltrichlorosilane and decyltrichlorosilane on the silicon substrates. Here we use an alternative approach, a two-step process involving a subsequent reaction of the partially modified surface by tris(TMS) with the silane carrying initiating sites, 3-(2-bromoisobutyryl)propyl dimethylethoxysilane. Intuitively, the individual reactions using single components should be more controllable and reproducible, yielding more ordered and better packed monolayers, than the competitive chemisorption using mixed silanes [39]. The control of the nanoscopic spatial distribution of the surface-tethered polymer brushes should also be effective.

To test the ability to control the growth of polymer brushes, the SIP was first conducted on the silicon-supported α-bromoisobutyrate monolayer. As measured by ellipsometry, the thickness of the α-bromoisobutyrate monolayers was 9.3 ± 0.1 Å. Fig. 1 shows the development of PMPC and P*t*-BMA thickness as a function of time at a targeted degree of polymerization (DP) of 200. Obviously, the thickness increased with time, suggesting that polymerization time can be used as a tool for controlling the growth of polymer brushes. The formation of polymer brushes was also verified by contact angle analysis. According to Fig. 2, both advancing (θ_A) and receding (θ_R) water contact angles of the silicon-supported α-bromoisobutyrate monolayer drastically changed from 72°/68° to ~20°/1° for the hydrophilic silicon-supported PMPC brushes and to ~100°/80° for the hydrophobic silicon-supported P*t*-BMA brushes

Previous work reported by Ejaz and co-workers [40] has demonstrated that the molecular weight of "free" polymer formed in the solution from the "sacrificial" or "added" initiator closely resembled that of the grafted polymer brushes cleaved from the surface. Thus, it can be used to monitor the SIP process. The fact that the molecular weight increases linearly with polymerization time and the molecular weight distribution is close to 1.0 for both PMPC and P*t*-BMA (data not shown) suggested that the polymerization was well controlled and the mechanism is living. The molecular weight ($\overline{M}_n$) of free polymer together with the ellipsometric thickness (t) of the grafted polymer brushes can be used to estimate the graft density (σ), which is the inverse of cross-sectional area (A_x) per chain of polymer brushes:

$$\sigma = \frac{1}{A_x} = \frac{t\rho N_A}{M}, \tag{3}$$

where ρ is the mass density (1.30 g/cm^3 for PMPC and 1.10 g/cm^3 for P*t*-BMA) and N_A is the Avogadro number. Using slopes obtained from the plots in Fig. 3, which correspond to t/M, the calculated graft densities of PMPC and P*t*-BMA brushes for the targeted DP = 200 are 0.46 and 0.25 chains/nm^2, respectively. Although dimethylethoxysilane was used for the preparation of the surface-tethered initiator, the graft density of the polymer brushes obtained from our studies are in the same range as the graft density of the polymer brushes prepared by surface-initiated ATRP using trichlorosilane for the preparation of the surface-tethered initiator (0.1 to 0.6 chains/nm^2) [11,13,35].

This part of the investigation has demonstrated that the formation of both PMPC and P*t*-BMA brushes by SIP from the surface bearing a α-bromoisobutyrate monolayer via the ATRP mechanism can be well controlled in terms of thickness, molecular weight, and molecular weight distribution, and the polymerization process is living.

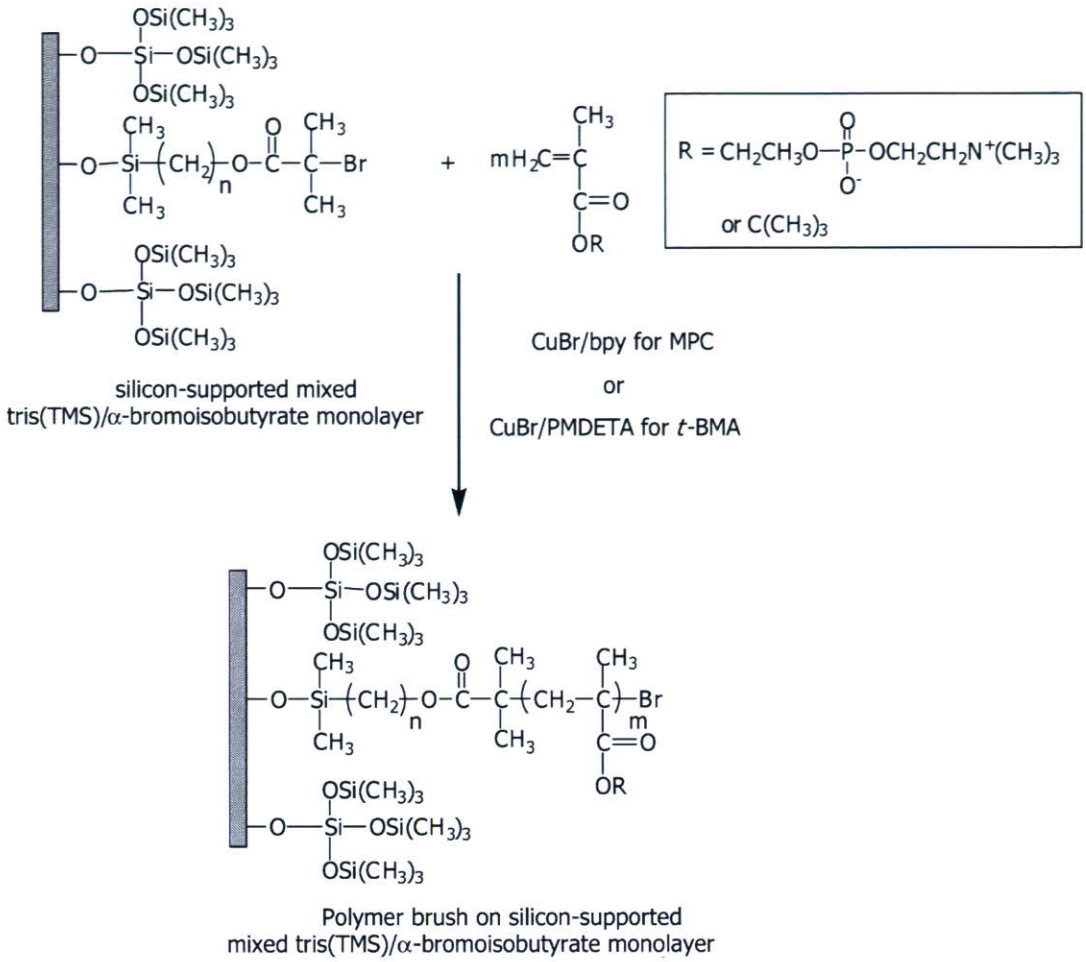

Scheme 2. Surface-initiated polymerization on silicon-supported mixed tris(TMS)/α-bromoisobutyrate monolayer.

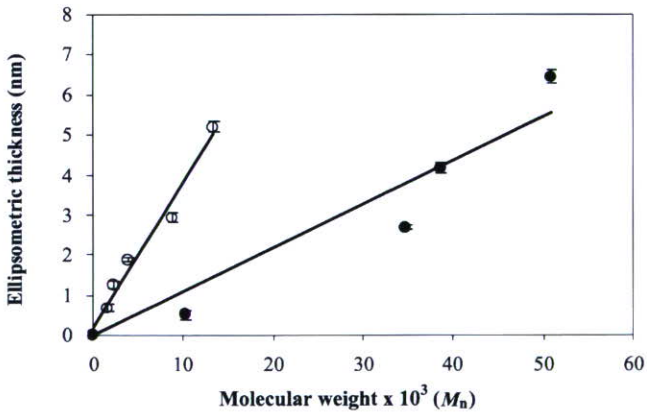

Fig. 3. Relationship between the ellipsometric thickness of polymer brushes and the molecular weight ($\bar{M}_n$) of free (●) PMPC and (○) P*t*-BMA.

3.3. Surface-initiated polymerization on silicon-supported mixed tris(TMS)/α-bromoisobutyrate monolayers

The silicon-supported mixed tris(TMS)/α-bromoisobutyrate monolayers was intended to be used as a nanoscale template for the formation of polymer brushes (Scheme 2). The growth of polymer brushes as a function of %tris(TMS) coverage and polymerization time is primarily discussed in terms of water contact angle and ellipsometric thickness. Using 5 h of polymerization, the thickness of PMPC and P*t*-BMA brushes, which is related to the density and length of polymer brushes, decreased as the %tris(TMS) coverage increased (Fig. 4). In contrast, the advancing and receding water contact angles of the mixed tris(TMS)/PMPC brushes shown in Fig. 5 proportionally increase with %tris(TMS) coverage. As a consequence of comparable hydrophobicity between the tris(TMS) monolayer ($\theta_A/\theta_R = 92°/82°$) and P*t*-BMA ($\theta_A/\theta_R = 100°/80°$), the water contact angle of the grafted P*t*-BMA brushes grown from the tris(TMS)/α-bromoisobutyrate monolayer was almost independent of %tris(TMS) coverage. It should be noted that the growth of polymer brushes from nanopores can also be tuned by the polymerization time (data not shown).

Originally, the observation that a surface having a certain %tris(TMS) coverage (~15–20 Å) is relatively thicker than an α-bromoisobutyrate monolayer (~10 Å) brought a concern that the short alkyl spacer between the surface-immobilized end and the other end bearing the α-bromoisobutyrate group, especially for $n = 3$, might be buried in the nanopores surrounded by tris(TMS) and unable to initiate polymerization. Although

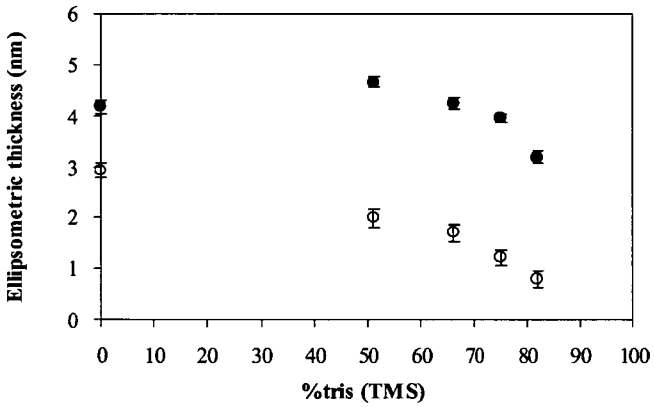

Fig. 4. Ellipsometric thickness of (●) PMPC and (○) P*t*-BMA brushes grown from the silicon-supported mixed tris(TMS)/α-bromoisobutyrate monolayer using a polymerization time of 5 h as a function of tris(TMS) coverage.

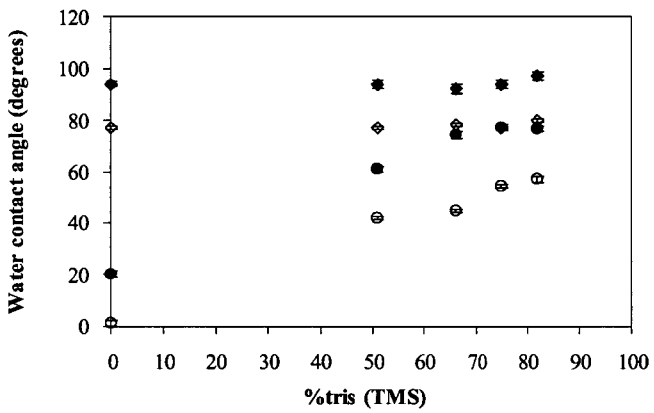

Fig. 5. Water contact angle of polymer brushes grown from the silicon-supported mixed tris(TMS)/α-bromoisobutyrate monolayer using a polymerization time of 5 h as a function of tris(TMS) coverage: PMPC: (●) θ_A, (○) θ_R and P*t*-BMA: (◆) θ_A, (◇) θ_R.

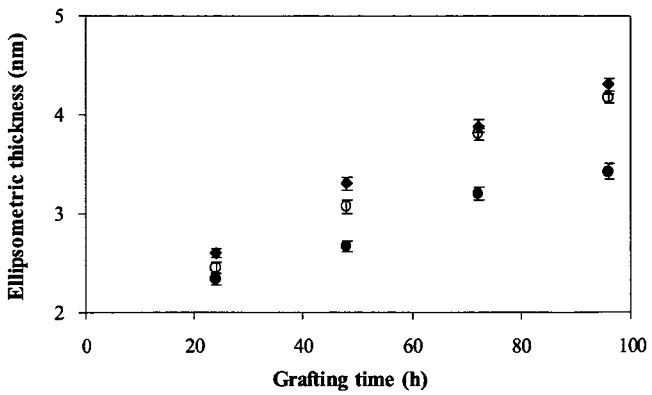

Fig. 6. Ellipsometric thickness of PMPC brushes grown from silicon-supported mixed 82% tris(TMS)/α-bromoisobutyrate monolayers versus grafting time of initiator using polymerization time of 5 h: (●) n_3, (○) n_6, and (◆) n_{10}.

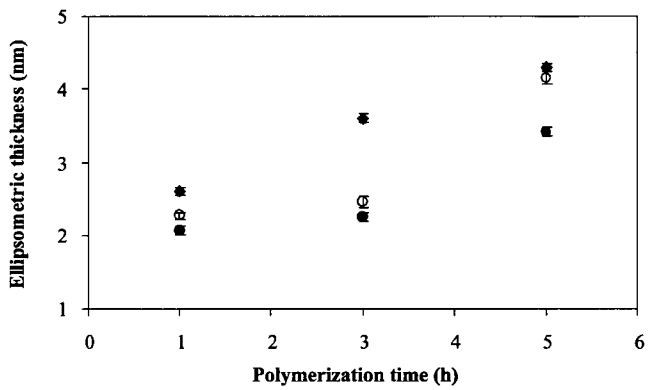

Fig. 7. Ellipsometric thickness of PMPC brushes grown from silicon-supported mixed 82% tris(TMS)/α-bromoisobutyrate monolayers versus polymerization time using grafting time of initiator of 96 h: (●) n_3, (○) n_6, and (◆) n_{10}.

the evidence shown above suggested otherwise, we still attempted to use two more analogous series of end-functionalized α-bromoisobutyrate silane compounds having longer spacers ($n = 6$ and 10) to react with the residual silanols in nanopores in order to determine the effect of the alkyl spacer on the efficiency of SIP. The immobilized α-bromoisobutyrate initiator is defined according to its alkyl spacer, denoting propyl ($n = 3$), hexyl ($n = 6$) and decyl ($n = 10$) as n_3, n_6, and n_{10}, respectively. The ellipsometric thicknesses of the silicon-supported α-bromoisobutyrate monolayers of n_6 and n_{10} are 15 and 18 Å, respectively.

Fig. 6 depicts the thickness of PMPC brushes grown from the silicon-supported mixed tris(TMS)/α-bromoisobutyrate monolayer having 82% tris(TMS) coverage. The density of the surface-tethered initiator was varied as function of grafting time in the range of 24–96 h. Polymerization was then carried out for 5 h. For a similar graft density of initiator (using the same grafting time), the thicknesses of PMPC brushes grown from n_6 and n_{10} are higher than those of PMPC brushes grown from n_3. This outcome can possibly be explained by the better mobility and the longer alkyl spacer of n_6 and n_{10}, allowing them to overcome the steric hindrance of the surrounding tris(TMS) and to reach monomers more efficiently than n_3. It can also be observed that the higher the graft density or the longer the grafting time of initiator, the denser and the thicker the PMPC brushes.

Using the grafting time of 96 h for all three initiators, the kinetics of surface-initiated polymerization of MPC on silicon-supported mixed tris(TMS)/α-bromoisobutyrate monolayers (n_3, n_6, and n_{10}) having 82% tris(TMS) coverage were determined. The thickness of PMPC brushes as a function of polymerization time is illustrated in Fig. 7. These data clearly suggest that not only does the alkyl spacer influence the ability of α-bromoisobutyrate to react with the monomers but also how fast it can react. The data points at 3 h can distinguish between the kinetics of n_6 and n_{10} at an early stage of polymerization. Nonetheless, such dissimilarity is no longer noticeable after a longer polymerization time.

3.4. Surface topography of polymer brushes in nanopores

AFM was used as a tool to monitor the surface topography of the grafted polymer brushes on the silicon-supported mixed tris(TMS)/α-bromoisobutyrate monolayer. In comparison with a clean substrate, the modified surfaces bearing

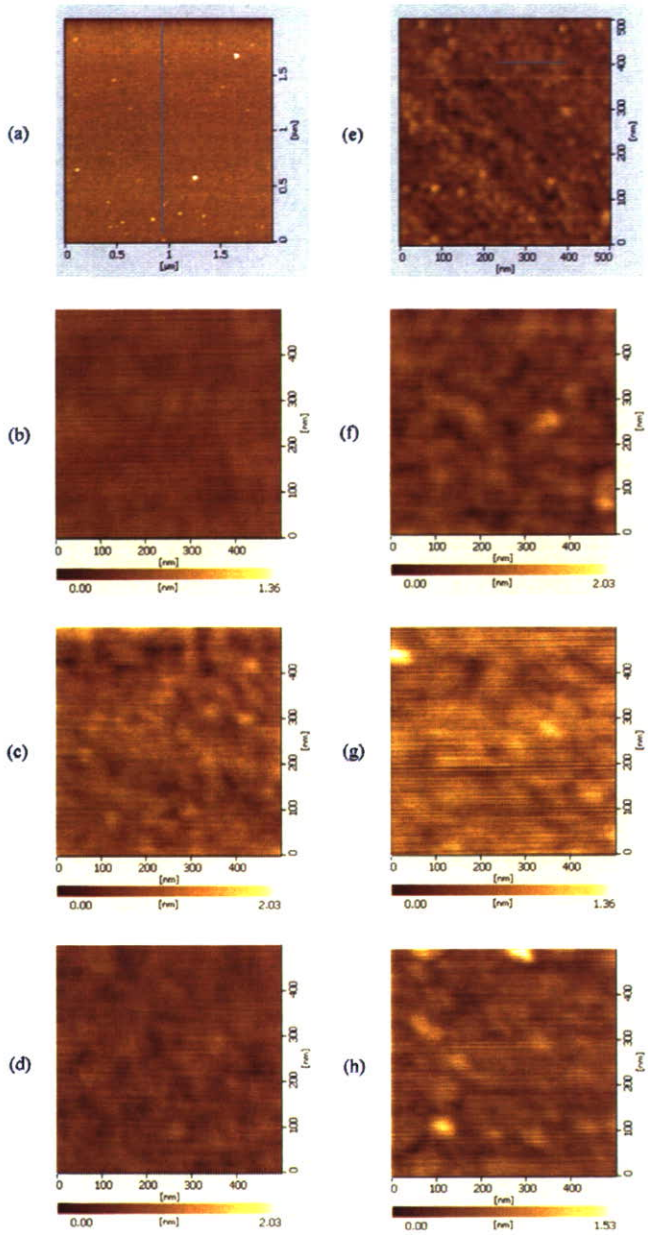

Fig. 8. AFM images of the silicon-supported mixed tris(TMS)/silanol monolayer having varied %tris(TMS) coverage: (a) 0, (b) 51, (c) 66, and (d) 82% and the silicon-supported mixed tris(TMS)/α-bromoisobutyrate monolayer having varied %tris(TMS) coverage: (e) 0, (f) 51, (g) 66, and (h) 82%.

a tris(TMS)/silanol monolayer were almost featureless and relatively smooth (Fig. 8). Average roughnesses (R_a) of all modified substrates are listed in Table 3. Evidently, the coverage of neither tris(TMS) alone nor the tris(TMS) and α-bromoisobutyrate significantly altered overall surface roughness. In order to investigate the spatial distribution of PMPC brushes, the silicon-supported mixed tris(TMS)/silanol surfaces having various percentages of the tris(TMS) coverage were used as nanoscale templates for surface-initiated polymerization. The graft density of surface-tethered α-bromoisobutyrate groups was also varied as a function of reaction time between

Table 3
Average roughness (R_a) of the silicon-supported mixed surfaces determined by AFM analysis

%tris(TMS) coverage	R_a (nm)	
	Silicon-supported mixed tris(TMS)/silanol monolayer	Silicon-supported mixed tris(TMS)/α-bromoisobutyrate monolayer
0	0.2006	0.1708
51	0.0794	0.1322
66	0.1174	0.1401
82	0.0954	0.1508

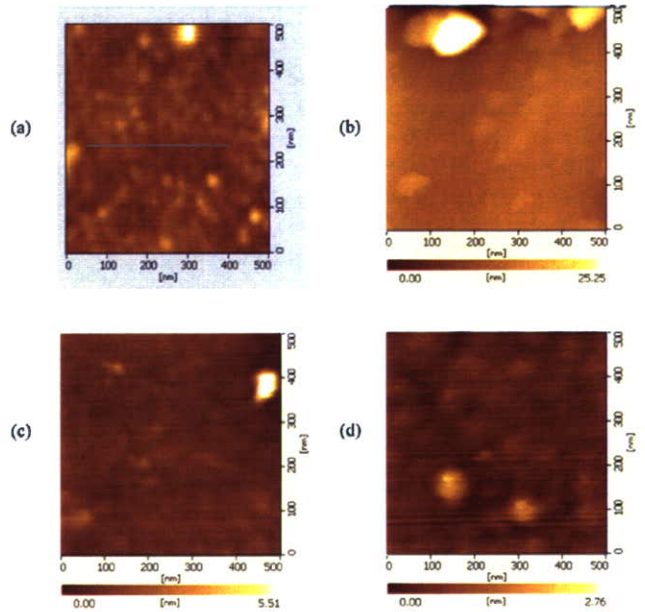

Fig. 9. AFM images of the silicon-supported mixed tris(TMS)/PMPC brushes having varied %tris(TMS) coverage: (a) 0, (b) 51, (c) 66, and (d) 82%.

the residual silanol groups in nanopores with the silane compound having end-functionalized α-bromoisobutyrate groups (n_3).

First, an effect of %tris(TMS) coverage on topography of surfaces having grafted PMPC brushes was explored. Using 96 h of reaction time between the silicon-supported mixed tris(TMS)/silanol monolayers and the silane compound, it was assumed that the residual silanols in nanopores are completely replaced by the α-bromoisobutyrate groups that are capable of initiating polymerization. In other words, the nanopores are mostly filled with surface-tethered initiator and there was not much space between the grafted initiators and the surrounding tris(TMS) groups. Originally, we envisioned that protrusions representing the aggregates of PMPC brushes in the nanopores should appear on the surface and the higher the %tris(TMS) coverage, the smaller the size of protrusions. AFM images of the silicon-supported mixed tris(TMS)/PMPC brushes having different %tris(TMS) coverage using the polymerization time of 1 h, shown in Fig. 9, suggest otherwise. None of the surfaces showed any features that could be evidence of a nanoscopic distribution of PMPC brushes grown from the nanopores, even

Table 4
Average roughness (R_a) of the silicon-supported mixed tris(TMS)/PMPC brushes determined by AFM analysis

%tris(TMS) coverage	R_a (nm)	
	Polymerization time of 1 h	Polymerization time of 5 h
0	0.1783	0.1322
51	0.4660	0.1598
66	0.2359	0.1727
82	0.1398	0.1404

though the silicon-supported mixed tris(TMS)/PMPC brushes having 51% tris(TMS) coverage exhibit higher roughness than the others. According to the data in Table 4, the surfaces became even smoother after a longer period of polymerization (5 h) was used.

We postulate that the densely grafted PMPC brushes within the limited space in the nanopores may be forced by the surrounding tris(TMS) to stretch away from the surface when the polymer chain is relatively short and densely packed inside the nanopores. After a sufficiently long period of polymerization, the polymer chains became so long that they can no longer stretch out, thereby tending to fold over the tris(TMS) monolayer. For that reason, the surface assumes a relatively smooth topography in spite of its low overall graft density in the presence of tris(TMS). That was exactly observed in Fig. 9. Nonetheless, the surfaces may become increasingly rougher if extensive growth of polymer brushes is allowed (polymerization time >5 h).

To visualize the evolution of PMPC brushes grown from nanopores, two alternative routes were undertaken in order to regulate the graft density of PMPC brushes. First, by fixing %tris(TMS) coverage at 82%, one strategy exploited the kinetic control over the reaction between the silicon-supported mixed tris(TMS)/silanol monolayers and the silane compound from 24 to 96 h, which later yielded a low to high graft density of initiator and corresponding PMPC brushes. According to Fig. 10, it was found that the surfaces having varied graft density of PMPC brushes exhibited protrusions having a diameter of less than 100 nm. The size of the protrusions was in good agreement with the average roughness (R_a) listed under each image. The protrusions are believed to represent self-aggregation of PMPC brushes in nanopores. In the case of a low graft density (Fig. 11), there should be enough space within the pores for the polymer chains to adopt a more coil-like architecture or aggregated form (mushroom regime) instead of being in extended forms (brush regime), which are thermodynamically unfavorable. As the packing of PMPC brushes was denser, the protrusions became larger and so did the roughness. The phase separation that led to the PMPC brushes aggregation was believed to be further driven by the different hydrophilicity/hydrophobicity between the PMPC brushes and the surrounding tris(TMS).

Assuming that there is no lateral broadening due to the AFM tip shape, the average number of chains within one of the protrusion can be estimated. First, the volume occupied by one PMPC chain (V_{mol}) was determined using the following equation:

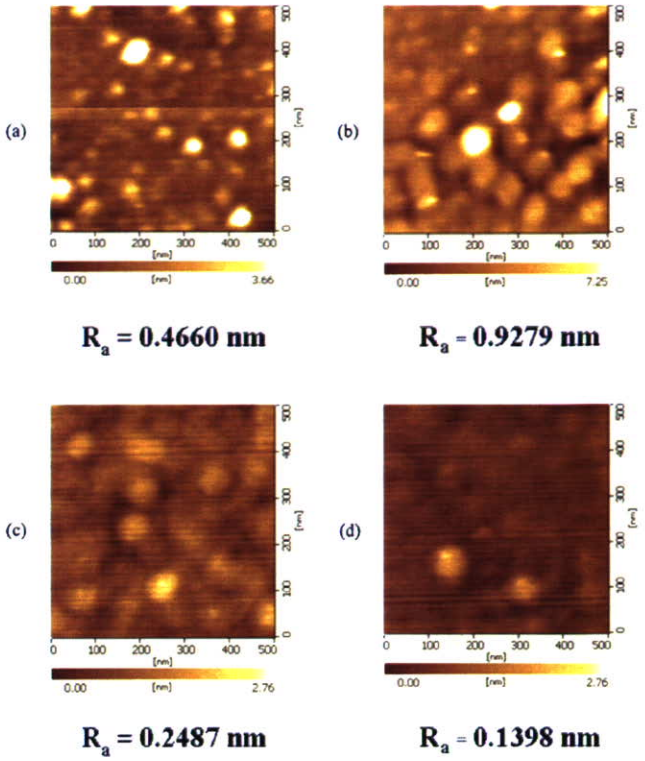

Fig. 10. AFM images of the silicon-supported mixed 82% tris(TMS)/PMPC brushes, controlling the grafting time of initiator: (a) 24, (b) 48, (c) 72, and (d) 96 h.

$$V_{mol} = \frac{M}{\rho N_A}, \tag{4}$$

where the bulk density (ρ) of PMPC is 1.30 g/cm^3 and N_A is the Avogadro number. Using the polymerization time of 1 h and the MPC:added initiator of 200:1, the PMPC molecular weight obtained by GPC analysis is 24,248 g/mol and the calculated V_{mol} is 31 nm^3. From the diameters (d) of the protrusions seen in Figs. 10a–10c which is varied in the range of 30–80 nm, the average volume of the protrusion (V) assuming the shape of a cylindrical disk can be calculated by

$$V = \frac{\pi d^2 h}{4}, \tag{5}$$

where h is the height of the protrusion. The height estimated from AFM image (data not shown) is 1.0 and 1.5 nm for the protrusion having the diameter of 30 and 80 nm, respectively. It turns out that the average volume of the observed protrusions is between 7.1×10^2 and 7.5×10^3 nm^3 which correspond to 23–242 chains. Having the same tris(TMS) coverage (~80%), Stafford and co-workers [27] can only incorporate 5 chains of PS–COOH in the nanopores. These numbers are reasonable considering the fact that we used the "grafting from" method as opposed to their "grafting to" method. To calculate the surface density of the protrusions, the number of chains was divided by the area of the protrusion ($\pi(d/2)^2$). The surface density of the protrusion within the nanopores is varied in the range of 0.02–0.05 chains/nm^2. As expected, these values are well below the